ADDIS ABABA UNIVERSITY

SCHOOL OF GRADUATES STUDIES

DEPARTMENT OF ERATH SCIENCES

ESTIMATION OF EVAPOTRANSPIRATION AND BIOMASS PRODUCTION USING REMOTE SENSING TECHNIQUES IN LAKE ZIWAY CATCHMENT

A THESIS SUBMITTED TO THE SCHOOL OF GRADUATE STUDIES IN PARTIAL FULFILLMENT FOR THE DEGREE OF MASTER OF SCIENCE IN REMOTE SENSING AND GIS

BINIAM TESHALE BEYENE

December 2007

b

Addis Ababa University

School Of Graduates Studies

Estimation of Evapotranspiration and Biomass Production Using Remote Sensing Techniques in Lake Ziway Catchment

By

Biniam Teshale Beyene

Remote Sensing and GIS Unit

Department Of Earth Sciences

Faculty Of Science,

Addis Ababa University

Approval by Board of Examiners

Dr. Balemual Atnafu _____
Chairman, Department
Graduate Committee

DR. Dagnachew Legesse _____
Advisor

Dr.Tenalem Ayenew _____
Examiner

Dr. K.V. Suryabhagavan _____

Examiner

Declaration

I the undersigned, declare that this thesis entitled "**Estimation Of Evapotranspiration And Biomass Production Using Remote Sensing Techniques In Lake Ziway Catchment**" is my work and that all sources of the materials used for the thesis have been duly acknowledged. I further declare that this work has not been submitted to any other University or Institution for the award of any degree or diploma.

Name: - Biniam Teshale

Place: - Addis Ababa University, Addis Ababa

Signature_____

Date_____

This thesis entitled "**Estimation Of Evapotranspiration And Biomass Production Using Remote Sensing Techniques In Lake Ziway Catchment**" is an original work by Biniam Teshale under my supervision.

Name: DR. Dagnachew Legesse

Signature_____

Date_____

Acknowledgements

First of all, I would like to thank 'My Almighty **God**' who made it every thing possible.

A particular debt of thanks to Dr. Dagnachew Legesse, Department Head of Remote Sensing and Geographic Information System in Earth Science, Addis Ababa University for his effort on guidance and encouragement.

I like to thank all members of the Earth science department, throughout the gestation period of the thesis, thanks also to National Meteorological Agency.

Finally, I am grateful to my family and a big thanks to all my friends and colleagues contribute to the study through their ideas, comments and suggestion.

Table of contents

List of tables

Page

List of figures

Page

List of plates

Page

List of annexes

List of acronyms

a_s Fraction of extraterrestrial radiation reaching the earth on an overcast day [-]

$a_s + b_s$ Fraction of extraterrestrial radiation reaching the earth on a clear day [-]

Cn n number of carbon

cp Specific heat [MJ kg-1 °C-1]

dr Inverse relative distance

E Evaporation [mm day-1]

Epan Pan evaporation [mm day-1]

e°(T) Saturation vapour pressure at air temperature T [kPa]

es Saturation vapor pressure for a given time period [kPa]

ea Actual vapour pressure [kPa]

ET Evapotranspiration [mm day-1]

ETo Reference crop evapotranspiration [mm day-1]

G Soil heat flux [MJ m-2 day-1]

Gsc Solar constant = 0.0820 MJ m^{-2} min^{-1} ,

H Sensible heat [MJ m-2 day-1]

Hrs Hours

Lst Local time

LAI Active (sunlit) leaf area index [-]

m.a.s.l Mean above sea level

ppm Part per million

Ra Extraterrestrial radiation [MJ m-2 day-1]

Rl Long wave radiation [MJ m-2 day-1]

Rn Net radiation [MJ m-2 day-1]

Rnl Net long wave radiation [MJ m-2 day-1]

Rns Net solar or shortwave radiation [MJ m-2 day-1]

Rs Solar or shortwave radiation [MJ m-2 day-1]

r_{ah} Aerodynamic resistance [s m-1]

r_s Bulk surface or canopy resistance [s m-1]

RH Relative humidity [%]

T Air temperature [°C]

u2 Wind speed at 2 m above ground surface [m s-1]

ώs Sunset hour angle

Φ Latitude (rad)

δ Represents solar declination (rad)

ε' Maximum conversion factor for above ground biomass

Λ Evaporation fraction

Abstract

Estimation of actual evapotranspiration and biomass production require accurate real circumstances, i.e. for heterogeneous terrain composed of various agroecosystems under erratic rainfall patterns, sparse canopies, and imperfectly managed drainage systems. Hence, it is necessary to evaluate whether the current conventional methods can estimate the actual evapotranspiration and biomass production frequently with accurate measurement from limited meteorological data. This study shows surface energy balance algorithm (SEBAL) method used to compute actual evapotranspiration and biomass production in Central Main Ethiopian Rift System and adjacent highlands of Lake Ziway catchment.

Actual evapotranspiration and biomass production maps have been generated for the year 2004 and 2005 respectively. The results of this study show that daily actual evapotranspiration lies in the range between 0.7 and 8 mm/day, in which the spatial variability of daily actual evapotranspiration were demonstrated. Monthly actual evapotranspiration was ranging from 27 to 250 mm/month. This also suggests that the spatiotemporal variability of monthly actual evapotranspiration through out the seasons occurred. Moreover, in SEBAL analyses dry biomass production over traditionally cultivated farm lands was 150 Kg/ha on average whereas dry biomass production increases during the late crop growing stage. Therefore, It is concluded that the remotely sensing energy balance model, such as SEBAL can be used to retrieve important crop parameters of actual evapotranspiration and biomass production.

Introduction

1.1. Background

Water is an essence of food and the basic component of life. Fresh water has become a major source for domestic and agricultural uses from the available existing surface water and ground water in the environment like the Main Ethiopia Rift System .The Main Ethiopia Rift System mostly known with its diverse hydrological environment where number of rift lakes including lake Ziway characterized by a chain of lakes varying in size, hydrological and hydrogeological. According to Dagnachew Legesse (2003), currently improper utilization of water resources in the rift resulted substantial changes on the environment due to climate and land use changes.

Especially, in the study area (Ziway catchement), the most important large-scale withdrawals of water are related to irrigation activities due to the high population growth puts a great demand for food.

An understanding of Spatial and temporal variation of parameters including surface albedo, surface temperature, evapotranspiration (ET), solar radiation and rainfall are important in development management strategy for efficient use for available water resources. Digital maps of actual evapotranspiration indicate that depletion of water resources enables policymakers to address the issue of consumption water use, including beneficial and no beneficial depletions. Estimation of actual evapotranspiration is a complex task to quantify in catchement scale. Solar energy source, Electromagnetic Radiation (EMR) absorbed by surface features which undergo evaporation process from moist soil, water held in the pores space of rock and water bodies. Hence, the interaction of EMR with vegetation which is known as transpiration in which the process of vaporization of liquid water contained in plant tissue removed to the atmosphere to keep plant temperature to the response of thermal energy. Plant use solar energy to convert water and carbon dioxide to plant biomass through the process of photosynthesis.

In the estimation of spatio-temporal variations of important crop parameters such as actual evapotranspiration and the total dry organic matter or stored energy content of living organisms that is present in crop (biomass) were applied in the catchement using SEBAL model and satellite remote sensing techniques. Energy is detected by remote sensing technology in which how energy is distributed between its source and the material on its way across the atmosphere to the satellite detector were analyzed and interpreted.

SEBAL model require a minimum amount of meteorological data as inputs from the principal stations installed in the study area at Ziway on which meteorological parameters are recorded include air temperature in degrees Celsius (maximum and minimum), sunshine duration in hours radiation, wind speed in meters per second at 2 meters height recorded , calculated relative humidity (%) at 0600 Hrs (Lst), 1200 Hrs (Lst), and 1800 Hrs (Lst),and rainfall in millimeters per day even though principal stations at Bui and Kulumso are exist with limited time serious meteorological data. Moreover twelve point precipitation stations are installed in the catchement.

Therefore estimating crop parameters with satellite spectral data has the advantage that accessing the parameters being easy, fast and economical in the case of this particular study.

1.2. Statement of the problem

The Federal Democratic Republic of Ethiopia (FDRE) formulated an agricultural development policy by increasing the productivity of land through improved management of the available resources. In achieving the country's development strategy, knowledge on actual ET and biomass production computation are needed. Hence, it is necessary to evaluate whether the current conventional methods can estimate the crop parameters frequently with accurate measurement. In most of the meteorological stations the spatial distributions are not dense besides few are suffers from missing data, so conventional techniques have limitations to use their data for real time evaluation and analysis of crop parameters in the catchment .To estimate the actual ET and biomass growth, actual field data is needed, but unavoidable time delays in this process cause delays in the decision making process. In order to make decisions at the right time, the delays of acquiring and processing of field data should be minimized. So Satellite remote sensing can furnish data in an objective and unbiased manner.

1.3. Objective of the study

1.3.1. General objective

The objective of this study is to justify the use of the SEBAL model with remotely sensed data to estimate actual ET and biomass production and to assess the results sufficiently to support the decision makers.

1.3.2. Specific objective

- To estimate the Spatio-temporal variability of actual evapotranspiration in the catchment.
- Estimation of biomass production in various crops development stages in traditional cultivated farming lands.

1.4. Significance of the study

This study helps researchers and decision makers to avoid reliance only on field information at regional scale by demonstrating the potential of remote sensing and GIS technique, which provide information from satellite spectral data on water resource information like actual evapotranspiration and biomass production.

1.5. Scope of the study

This study estimates actual evapotranspiration (ET) and biomass production for the entire Ziway catchement in northern Abyata-Shala basin including January, February, march, May, June, July, October, November and December in the year of 2004 and July to October 2005 with spatial resolutions of 1000 meters at high temporal resolution using SEBAL model. The researcher choose only the above mentioned months since cloud covered images are discarded out of daily images of MODIS.

SEBAL is a remote sensing algorithm that estimates reference ET, potential ET and actual ET without prior information on the hydrological, water management and land cover situation. The energy balance was used because it represents four parameters include: net radiation(Rn), sensible heat flux(H) and soil heat flux(G), but other energy components are not considered because they have small fraction of daily net radiation like heat stored and released.

The projection of the moment time estimated parameters especially actual evapotranspiration from daily to monthly ,need routine meteorological elements mostly they shows gaps of data on uninstalled stations at higher topographic range (>3000 m.a.s.l). Therefore the periodic actual evapotranspiration estimation applied with extrapolation technique based on available meteorological data. While estimated biomass production consider on potential accumulation for carbon four (C_4) crop type only.

1.6. Methods and Materials

This study relies substantially on available images of the Moderate Satellite (MODIS) sensor on board of the Terra (mid-morning overpass) used with other sensor data in combination with remote sensing based energy balance model for evapotranspiration and biomass production with ERDAS 8.7 software manipulations with model builder function as shown in figure 2. Geographical Information System (GIS) has been used for data management of daily and monthly meteorological data obtained from Ethiopia Meteorological service. GIS spatial analyses were carried to interpolate point measured meteorological elements to convert into raster data model based on spatial averaging technique. Delineation of Catchment boundary, river drainage network and topographic hill shade were processed with Arcgis9.1 software from Shuttle Radar Topographic mission (SRTM) 30 meter resolution imagery. Moreover Topographic map of 1:50,000 scales were obtained from Ethiopia mapping Authority. Geo-referencing of none referenced MODIS land surface temperature imageries were run with image to image registration technique. The map projection used for entire dataset is UTM, Zone 37 with Spheroid_WGS 84, Datum _WGS 84.

Surface energy balance algorithm for land energy balance approach evaluation on the base of energy conservation law used as resolved in equation 1 with net available radiation applied at the scale of the catchement. Components of radiation available on the surface of earth can be visualized in figure 1 that the major source of energy supply is solar radiation reaches on surface across the atmosphere as a short wave and some are also converts into thermal radiation. The Surface Energy Balance Algorithm for Land (SEBAL) approach for computing actual evapotranspiration over the area is discussed in Section 6.

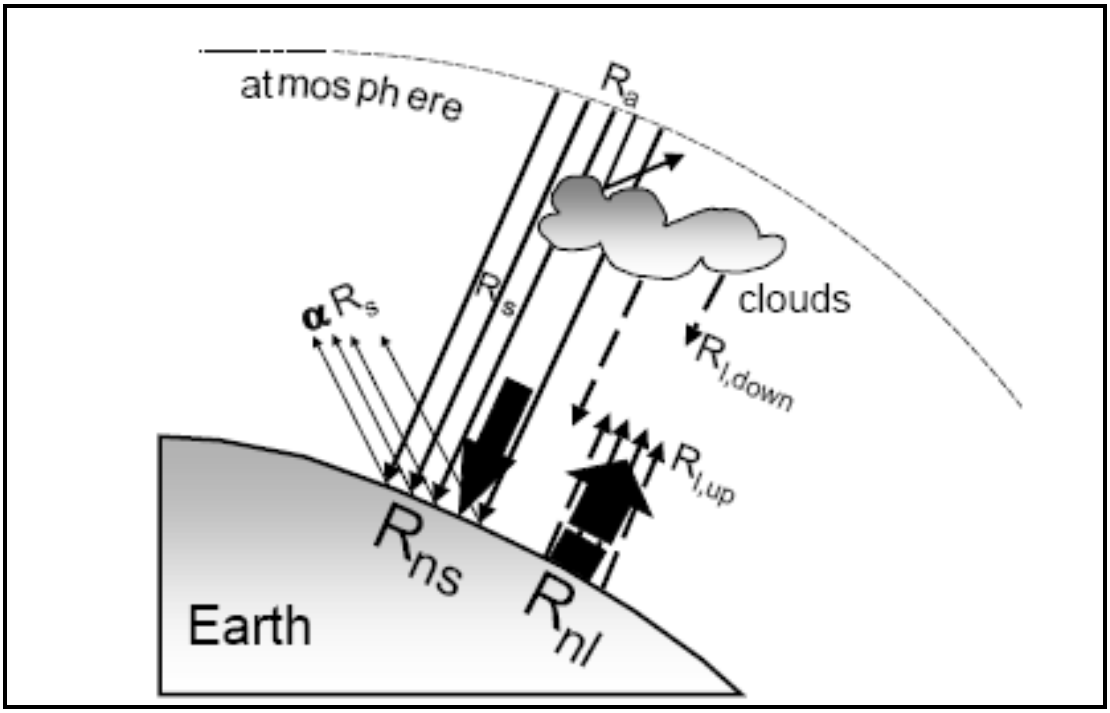

Figure 1 Component of net radiation

Net available radiation can be computer as follows

$$R_n = R_{s,down} - R_{s,up} + R_{L,down} - R_{L,up} \quad \text{Eq. (1)}$$

Where;

$R_{s,down}$: incoming short-wave radiation ($w.m^{-2}$), if it is not possible to measure in situ incoming short wave radiation it can be calculated with angstrom formula

$$R_{s,down} = (a_s + b_s \, .n/N)Ra \quad \text{Eq. (2)}$$

Where; Ra is extra atmospheric radiation (MJ m^{-2} day^{-1})

n is actual duration of sunshine (hour)

N is maximum possible duration of sunshine (hour)

n/N Represents sunshine duration.

a_s is regression constant, expressing the fraction of extra atmospheric Radiation reaching the earth on overcast days (n=0)

$a_s + b_s$ is fraction of extra atmospheric radiation reaching the earth on Clear sky (n=N).

An extraterrestrial radiation (Ra) for each day of the period and average latitude can be estimated as follows;

$$Ra = \frac{24(60)}{\Pi} . Gsc.dr\ (ώs \sin(\Phi) \sin(\delta) + \cos(\Phi) \cos(\delta) \sin(ώs)) \ldots\ldots Eq. (3)$$

Where;

Gsc ‘is solar constant = 0.0820 MJ m^{-2} min^{-1} , ‘ dr ‘ is inverse relative distance earth-sun.

ώs is sunset hour angle

Φ is latitude (rad)

δ represents solar declination (rad)

$\mathbf{R_{s,}}_{up}$: outgoing short- wave radiation ($w.m^{-2}$) depend on albedo and income radiation

$$Rup = \rho o. \mathbf{R_{s,}}_{down} \ldots\ldots Eq. (4)$$

ρo : albedo, the fraction of the total solar radiation incident on a body that is reflected by it was derived from composed of different 7 band reflection from MODIS imagery.

$\mathbf{R_{L,}}_{down}$: incoming long wave radiation which depends on the ratio of the radiation emitted by a surface to that emitted by a black body at the same temperature, emmisivity of atmosphere (ε) unit less can be extracted from Meteosat with the following relation

$$\varepsilon = (a_s + b_s .n/N) \ldots\ldots Eq. (5)$$

In case of a_s and b_s values are vary due to atmospheric condition and actual solar radiation along latitude and year of month so that values a_s and bs are 0.25 and 0.5 respectively are recommended.

Stefan-Boltzmann Law ($H= \sigma T^4$) where H is total radiation emittance per unit area in w/m^{-2} σ represent Stefan-Boltzmann constant (0.000000056 $W/m^2/K^4$) and T is absolute temperature in Kelvin (K)

$$\mathbf{R_{L,down}} = \sigma .\varepsilon. (T_{atmosphere})^4 \ldots\ldots\ldots\ldots\ldots\ldots\ldots\ldots\ldots\ldots\ldots\ldots\ldots\ldots \text{Eq. (6)}$$

$\mathbf{R_{L,up}}$; out going long wave radiation which depend on emmisivity(ε_o)of the surface and surface temperature(To) from MODIS11product available.

$$\mathbf{R_{L,up}} = \sigma .\varepsilon_o T_o^4 \ldots\ldots\ldots\ldots\ldots\ldots\ldots\ldots\ldots\ldots\ldots\ldots\ldots\ldots\ldots\ldots\ldots\ldots \text{Eq. (7)}$$

Equations 6 is simplified into the following equation

$$\mathbf{Rn} = (1- \rho o)\, \mathbf{R_{s,down}} + \sigma .\varepsilon. (T_{atmosphere})^4 - \sigma .\varepsilon_o T_o^4 - (1- \varepsilon_o)\, \sigma .\varepsilon. (T_{atmosphere})^4 \ldots \text{Eq.(8)}$$

The study of actual evapotranspiration is based on a spectral satellite data which acquired onboard shown in table 1 are measured optical and thermal characteristics of earth matter properties. Numbers of MODIS imageries which are on board of Terra satellite measurement from 36 channels were obtained from Redhook Eros data center internet web site using file transfer protocol. MODIS spectral bands of different spatial resolutions, including visible (band 1) and near infrared (band 2) bands is 250 m at satellite nadir and for both thermal bands (band 31 and 32) spatial resolution is 1000 m. However, the ultimate results are confined to the 1000 m resolution. Therefore the images of band 1 and band 2, which were pre-processed into the standard spatial resolution of 1000 m, were used for image analyses.

MODIS has been selected because of its thermal band for measuring land surface temperature. Another advantage for using MODIS is its very short return period (daily images of both Aqua and Terra) that allows proper temporal monitoring of rapid changes in crop development and water use.

Meteosat (Mission of second generation) of European space and aerodynamic exploration agent owned satellite have been used for estimation of short wave radiation reaches on surface of the earth with describing the presence of cloud which indicates the atmospheric transmittance of solar radiation with time (equation 2).

ASTER imagery used for identification of different land use and land cover type in the catchement with computer based image classification. Before interpretation, preprocessing of the images Geometric and Radiometric corrections were carried entirely over all data sets. Land use and land cover type first done with unsupervised classification with grouping multi-band spectral response pattern into clusters that is statistically separable. Thus, small number of pixel valued (DNs) can fix one cluster that is set apart from a specific range combination for another clusters and so forth on parameters given to separation. On the bases of the out put of unsupervised classification results, base map were prepared for field survey for reference ground truth data collection with an instrument of Global Positioning System (GPS) for specific land use and land cover type then assigned training area to train the computer and examine the data in each band and to sort out particular correlation among DNs can be assed as in the likelihood of the pixel to each training class given from GPS data with a method of maximum-likelihood of supervised classification. Supervised classified finally accepted because of more effectual in terms of accuracy in the mapping of land use and land cover types (figure 6).

SPOT Vegetation of NDVI (figure 14) times series data from June 2005 and November 2005 (3 composites per months) 1000 meters resolution have been used as an input to estimate dry biomass production results from above the surface due to leave system and underground due to rooting system of the plants.

The Shuttle Radar Topography Mission (SRTM) obtained elevation data on a near-global scale to generate the most complete high-resolution digital topographic database of the catchement including delineations of drainage system and the watershed. SRTM consisted of a specially modified radar system that flew onboard the Space Shuttle endeavor during an 11-day mission in February of 2000. SRTM is an international project spearheaded by the National Geospatial-Intelligence Agency (NGA), NASA, the Italian Space Agency (ASI) and the German Aerospace Center (DLR).

The concept of calculating net primary biomass production as a function of Absorbed Photo synthetically Active Radiation (APAR) determines by Bastiaanssen and Ali (2003) has given with the following relationships:

$$\text{Biomass} = \sum_{t=0}^{n} \varepsilon\, f(NDVI)\, 0.48\, R_{L,down} \quad \text{..... Eq. (9)}$$

Where; f (NDVI) is the function relating NDVI with f PAR and $\mathbf{R_{L,down}}$,a reduction factor.

$$\text{Reduction factor} = 1.257*NDVI - 0.161 \quad \text{.....Eq. (10)}$$

ε (g MJ-1) is the light use efficiency; define as the ratio of canopy net photosynthesis to incident PAR. The light use efficiency ε is expressed as:

$$\varepsilon = \varepsilon' T1\, T2\, \Lambda\, 4.15 \quad \text{.....Eq. (11)}$$

Where; ε' is a maximum conversion factor for above ground biomass, Λ is evaporation fraction from SEBAL model. When environmental conditions are optimal*, T1 and T2* can be expressed as

$$T1 = 0.8 + 0.02\, Topt - 0.0005\, T^2 opt \quad \text{..... Eq. (12)}$$

$$T2 = 1.185.\ (1/\exp 0.2\, Topt - 10 - Tmon)*1/1+ \exp(-0.3 Topt^{-10} + Tmon) \quad \text{.....Eq. (13)}$$

Where; Topt (in degree celsius) is the mean air temperature during the month of maximum leaf area index or NDVI development, Tmon (in degree celsius) is the mean monthly air temperature. The conversion factor ε' ranges 1.8 to 2.7 g MJ-1 Bastiaanssen and Ali (2003) for the C3 plants in which the Plants (e.g., soyabean, wheat, and cotton) whose carbon- fixation products have three carbon atoms per molecule. C3 plants show a greater increase in photosynthesis with a doubling of CO_2 concentration and less decrease in stomata conductance, which results in an increase in leaf-level water-use efficiency and C4 Plants (e.g., maize and sorghum) whose carbon fixation products have four carbon atoms per molecule. Compared with C3 plants, C4 plants show little photosynthetic response to increased CO_2 concentrations above 340 ppm but show a decrease in stomata

conductance, which results in an increase in photosynthetic water-use efficiency.

Display of all images are as the gray scaling and for representing the final results with three additive primary colors (red, green and blue) RGB color space are used .

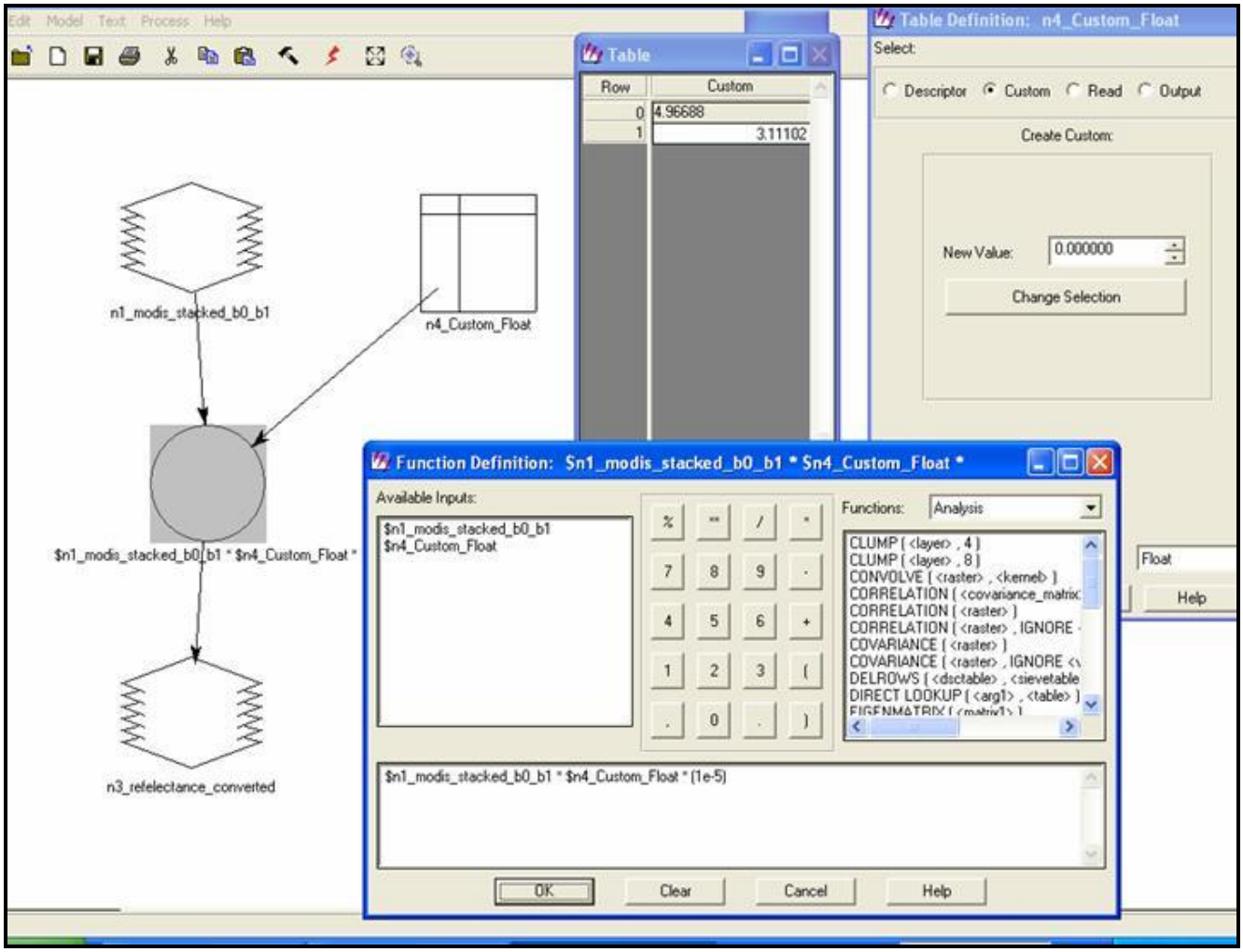

Figure 2 Model builders in ERDAS 8.7

Table 1 over view of different sensors

Type of Satellites	**Platform**	**Sensor**	**1st launch**	**Bands**	**Spatial resolution**	**Revisit period**
Meteorological Satellites	**Meteosat**		November 1977	Visible 0.45 - 1.0 µm Water vapor 5.7 - 7.1 µm Infrared 10.5 -12.5 µm	2.5 km 5 km 5 km	**30** min
Earth Resources Satellites	**Terra ASTER**	VNIR	March 2000	Band 1 (0.52 - 0.60) w/m^2/sr/µm Band 2 (0.63 - 0.69) w/m^2/sr/µm Band 3N (0.78 - 0.86) w/m^2/sr/µm Band 3B (0.78 - 0.86) w/m^2/sr/µm	15 meters	**16** days
		SWIR		Band 4 (1.600 - 1.700) w/m^2/sr/µm Band 5 (2.145 - 2.185) w/m^2/sr/µm Band 6 (2.185 - 2.225) w/m^2/sr/µm Band 7 (2.235 - 2.285) w/m^2/sr/µm Band 8 (2.295 - 2.365) w/m^2/sr/µm Band 9 (2.360 - 2.430) w/m^2/sr/µm Band 4 (1.600 - 1.700) w/m^2/sr/µm Band 5 (2.145 - 2.185) w/m^2/sr/µm Band 6 (2.185 - 2.225) w/m^2/sr/µm Band 7 (2.235 - 2.285) w/m^2/sr/µm	30 meters	
		TIR		Band 10 (8.125 - 8.475) w/m^2/sr/µm Band 11 (8.475 - 8.825) w/m^2/sr/µm Band 12 (8.925 - 9.275) w/m^2/sr/µm Band 13 (10.25 - 10.95) w/m^2/sr/µm Band 14 (10.95 - 11.65) w/m^2/sr/µm	90 Meters	

Type of Satellites	Platform	Sensor	1st launch	Bands	Spatial resolution	Revisit period
	SPOT	Vegetation	March 1988	0.43 - 0.47 µm (blue) 0.61 – 0.68 µm (red) 0.78 – 0.89 µm (near IR) 1.58 – 1.75 µm (mid IR)	1000meters	**26** days
Earth Resources Satellites	**MODIS**	Terra	March 2000	Band 1 620 – 670 nm Band 2 841 – 876 nm Band 3 459 – 479 nm Band 4 545 – 565 nm Band 5 1230 – 1250 nm Band 6 1628 – 1652 nm Band 7- 2105 – 2155 nm Band 8- Band 36	250meters 500 meters 1000meters	**1** to **2** days
	SRTM	C-band and X-band	February 2000	C-band and X-band	30meters 90meters 1Kilometre	stopped

2. Literature Review

A number of researchers have been conducted studies in the rift environment on a basin scale which contribute much to understand the environment. Different methods have been developed to estimate evapotranspiration process from remote sensing data, among them energy balance method using surface energy balance algorithm for land(SEBAL) were used in Ethiopian rift system and adjacent high lands to estimate actual evapotranspiration. It revealed that spatial and temporal variation derived from satellite based measurement meanwhile comparison were also made between the results from different method and it was found that an acceptable deviation according to Tenalem Ayenew (2003) . Following Bastiaanssen et al (2005) SEBAL model was validated over different environment found to be valid .One of the most important developments in the field of remote sensing hydrology is the determination of distributed aerial actual evapotranspiration from spectral satellite data, based on the energy balance approach developed with researchers Menenti (1984), Parodi (1993) and Bastiaanssen,(1995). Since the environment of Ziway-Shala basin is changing rapidly with the response of climatic and land use/land cover changes analyzed by Dagnachew Legesse (2002) through hydrological modeling provide to conceptualize the basin. The change in land use/land cover which is manifested by deforestation has negative effect on the hydrology of the catchement.

Tenalem Ayenew (1998) analyzed general hydrology and hydrogeology of Ziway-Shala basin and evaluated the water balance with equating different factors. Among the different factor actual ET were used to validate SEBAL results in this study. A reviewed also carried to understand the hydrogeological setting of the area in addition to regional geological with hydrogeological map of the rift valley Lake region published by Tesfaye Chernet (1982) .

Studies carried out by Gilabert and Melia (1990), Patel et al (1985) and Casanova et al. (1998) have shown viable relationships between spectral response of standard crop and its biomass. Monteith (1972) pioneered the concept of calculating net primary biomass production as a function of Absorbed Photosynthetically Active Radiation (APAR).

As evident indicated that growth rate of several agricultural crop are linearly increase with amount of biomass production and NDVI prince (1990). Experimental results have validated this concept for a number of crop types Kumar and Monteith (1981), Wigand et al (1989) and Casanova et al (1998). To determine the accumulation of biomass Bastiaanssen and Ali (2003) have given the empirical relationships with SEBAL model application from satellite based spectral data, are used for evaluation of biomass production in this study.

3. General description of the Ziway Catchement

3.1. Location of the study area

The study area: Ziway Lake and the surrounding high lands (Ziway catchement) are situated in the Central Main Ethiopia Rift System. This basin is stretched into Oromiya National Regional State where the eastern highland, volcanic peaks and Lake Ziway located and western highland are in the Southern Nation and Nationality People Region (figure 3). Ziway catchement is found at the Northern part of Ziway-Shala Basin and its geographical location extends from 7.39^0 and 8.51^0 latitudes and 38.19^0 and 39.4^0 longitudes. The study area covers Ziway Lake, Ketar and Meki sub-basins with total area coverage of 7,380 square kilometers.

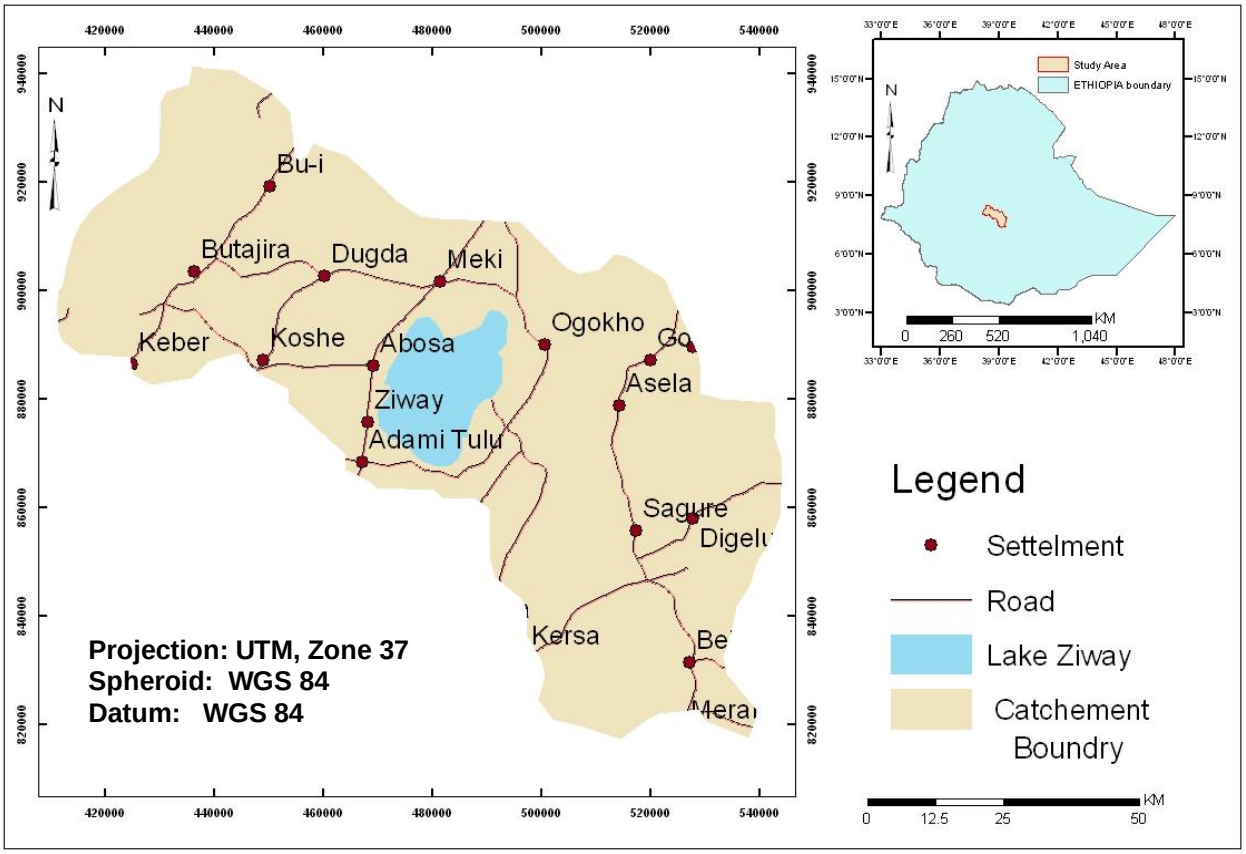

Figure 3 Location map of Ziway catchement.

3.2. Climate

The climate of the catchement is characterized by humid to sub – humid in the high lands while semiarid to arid type of climate found in the escarpment and rift floor. In the catchment bimodal and annual rainfall distribution patterns are experienced .The rain fall varies from 620mm in lower areas and increases to 1200mm on the average in the high lands of western and eastern parts. The temperature, humidity and wind speed are varying with different topographic setting in the catchment. The mean annual temperature also varies from 15 degree Celsius in the high lands and around 20 degree Celsius in the rift recorded at different meteorological stations.

3.3. Topography and Drainage

The Ziway catchement is part of Ziway-Shala basin. It includes sub-catchments of Meki and Ketar Rivers with surrounding Ziway lake area.

Topographically, Ziway catchment shows sharp variation. The central part of the digital elevation terrain (figure 4) shows that the rift floor with an average altitude of 1700 m.a.s.l in the vicinity to Lake Ziway. On the other hand the western and eastern high lands lie at range of 2000 – 3000 m.a.s.l; while peak volcanic ridges are found at North East of the catchment. To mention some of highest peaks includes Chilalo (4006 m.a.s.l), Galama (4225 m.a.s.l), Kakka(4001 m.a.s.l) and Guraga(3609 m.a.s.l).

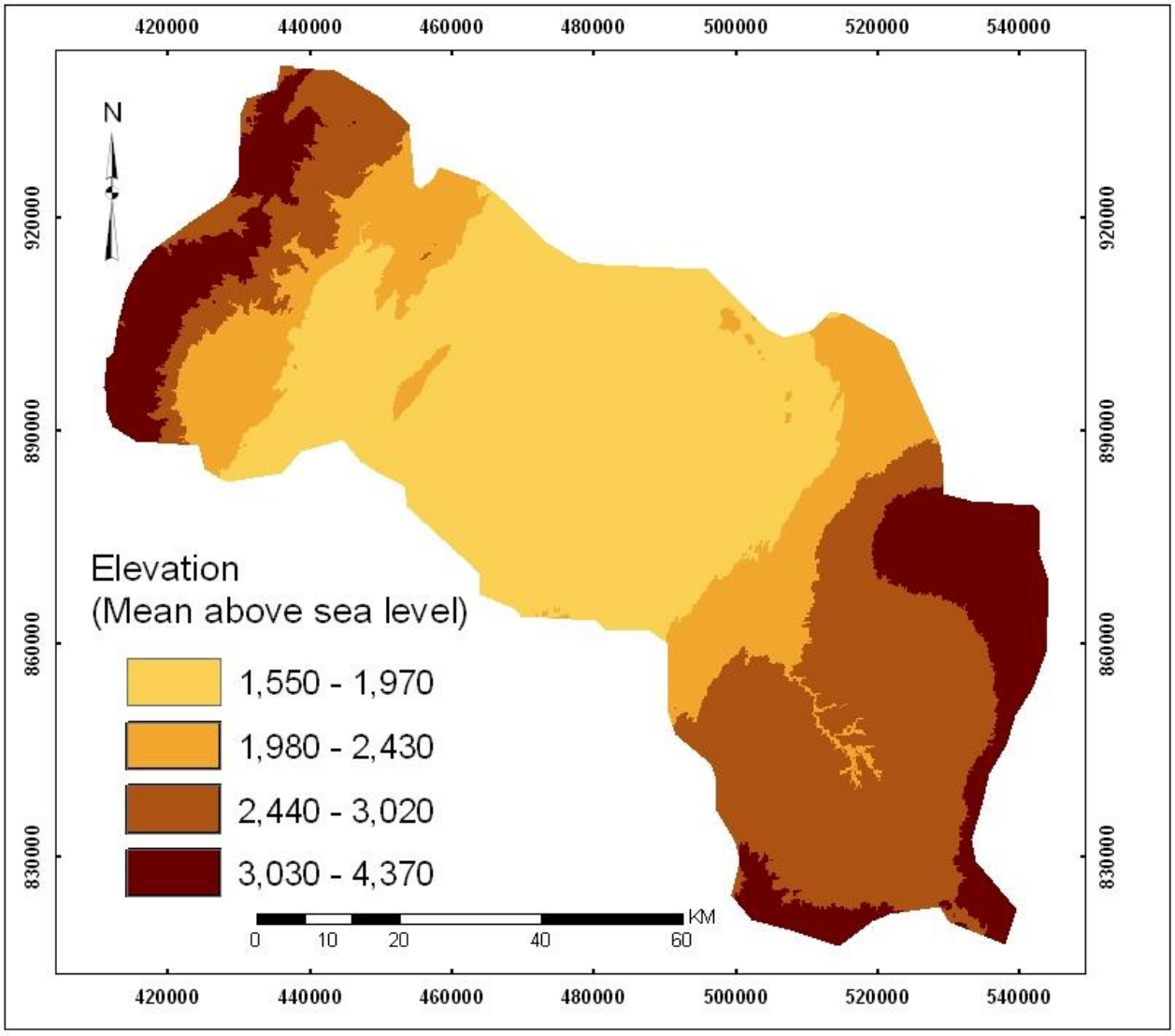

Figure 4 Topographic Map from SRTM 30 meter resolution imagery

The major rift valley lake exist in catchement at rift floor is Ziway lake as described in table 2 and the drainage networking displayed in figure 5 that the patterns of drainage formed following the slope of terrain and geological structure. Meki`s river tributaries starts from western high lands, they are short tributaries connected at angular almost seems 90 degree to longer straight major Meki River. Ketar`s river tributaries begin from eastern high lands are drained into common straight channel indicated the presence of geologically controlled system were developed.

Wetlands of Abaya are located at the western part of the catchement .Perennial wetlands also located east of Lake Ziway along Ketar River in which irrigation activities are carried on.

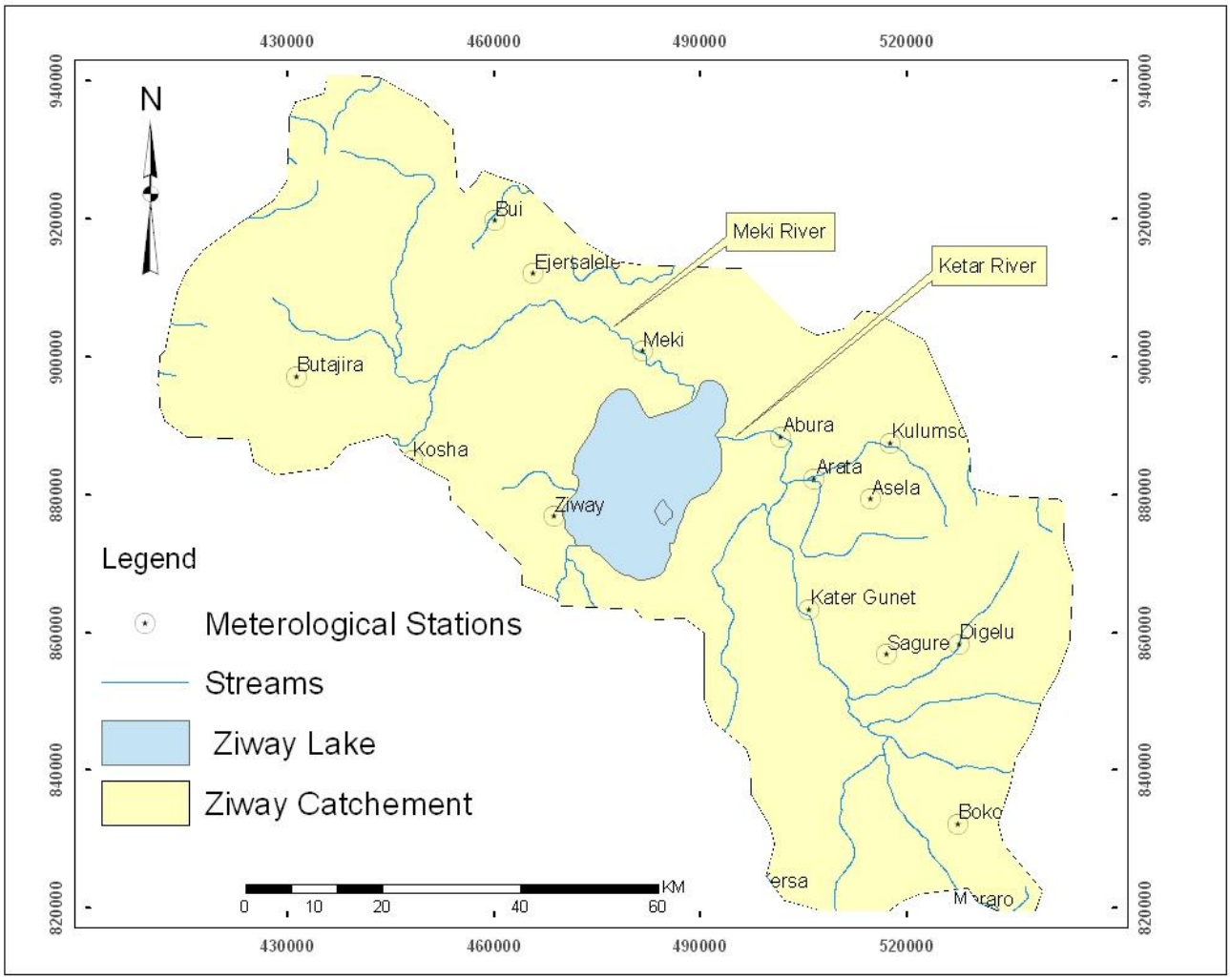

Figure 5 Drainage pattern and Meteorological stations map.

Table 2 Lakes data of in the studied basin.

Water body	Altitude(m.a.s.l)	Lake area	Catchement Area(Km^2)	Maximum depth(m)	Mean Depth(m)	Volume ($10^6 m^3$)
Ziway	1636	440	7380	8.9	2.5	1466

Source: Tenalem Ayenew(1998)

3.4. Land use and Land cover

Spatial distribution of land use and land cover types exist in the catchment as analyzed from January 2005 ASTER imagery using computer based classification with visual interpretation as in figure 6. Large area coverage occupied by intensively cultivated farm land lie on rift floor and plateau of high lands. Degraded forest due to deforestation for charcoal and land clearing for farming activities exist between 2000 and 3000 m.a.s.l, above which remnants of alpine mountain vegetation is covered.

The escarpment is also characterized by acacia and deciduous trees, and semi ever green bush lands. On the southern escarpment forest coverage exists where as the remaining highlands and the escarpment are farmlands with scattered trees and grazing lands.
Irrigation is the most obvious activity carried in the response to water scarcity in agricultural areas. Because it uses excessive water without considering the right time of watering including full irrigation activities involves in dry season around lake Ziway. Since the irrigation in this area is a year-round process, supplementary irrigation uses during variability in amount and duration of rainfalls. The Meki and Ketar rivers have been intensively used for irrigation activity. Onion, Tomato, Cabbage, Pepper, Sorghum and Maize are major crops grown in the basin. Several islands were mapped with in lake Ziway.

Recently, Floriculture (artificial cultivation of flowers using greenhouses) has become the dominant activity in the catchment. Major floriculture hotspots are around Lake Ziway (Plate1). Floriculture industry in the catchement is attracted due to favourable climate, abundant land, and water. Meanwhile it has an advantage in the following areas;

- Evapotranspiration rate decreases because the green house keeping the humidity cause water vapour not to be escaped.
- Increase agricultural product export diversification.
- Foreign exchange earning and employment generation.

As disadvantage of floriculture considered is introduction of significant quantities of agricultural chemicals in ground water resources and surface water pollution.

Plate 1 SherEthiopia (greenhouses)

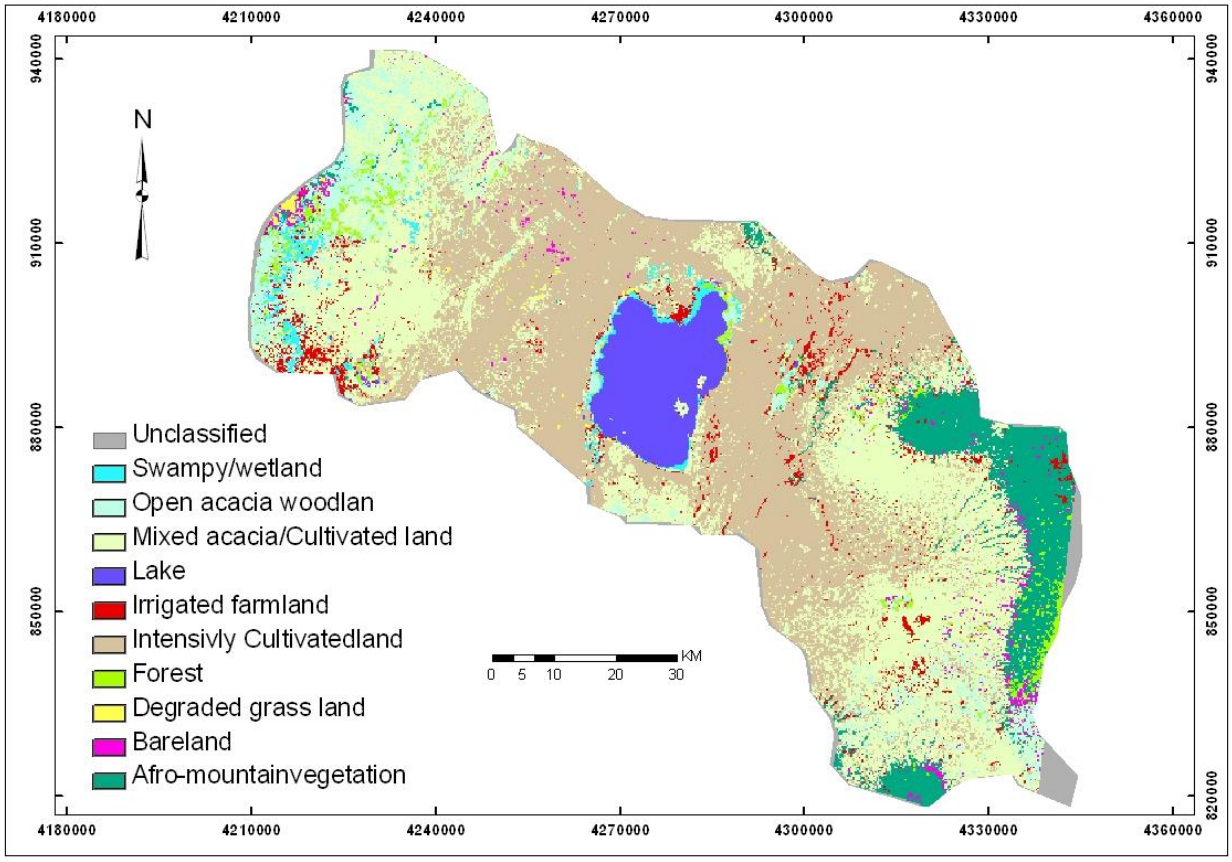

Figure 6 land use and land cover map.

3.5. Soil

In the catchement soil formation is closely related with the geology and degree of weathering. Basalt, ignimbrite, volcanic ash, pumice the main parent material to the formation of soil profile. Deeply weathered basalt in the humid highlands areas to unwearthed recent deposit in the dried central part of the rift system characterizes the degree of weathering.

Generally, there are four soil types in the area according to Makin et al (1976). Regosol/Lithosol type of soil is predominantly found in the eastern highlands of the catchment (figure7). It is characterized by well drained and limited moisture storing property, and bare stony outcrop. Eutric Nithosol is found within elevation range of 2000 to 3000 m.a.s.l at the South east and western part of the catchment. Vitric Andosol is found surrounding Lake Ziway in which it predominantly lacustrial sediment developed on the rift floor and on western escarpment of flat undulation plains with some hills formed on pyroclastic deposits. Generally, the soil have physical characteristics of dark grayish in color , free drainage, silty loam to sandy loam with moderate structure and good moisture storing property.

Finally Chromic/Eutric cambisol type of soil is found in the central part of the catchment which lies on steep faulted undulation and rolling low plateau escarpment of the rift zone this type of soil is well drained, moderately deep to deep dark gray or brown color, silty loam to sandy loam with moderate structure and good moisture storing properties.

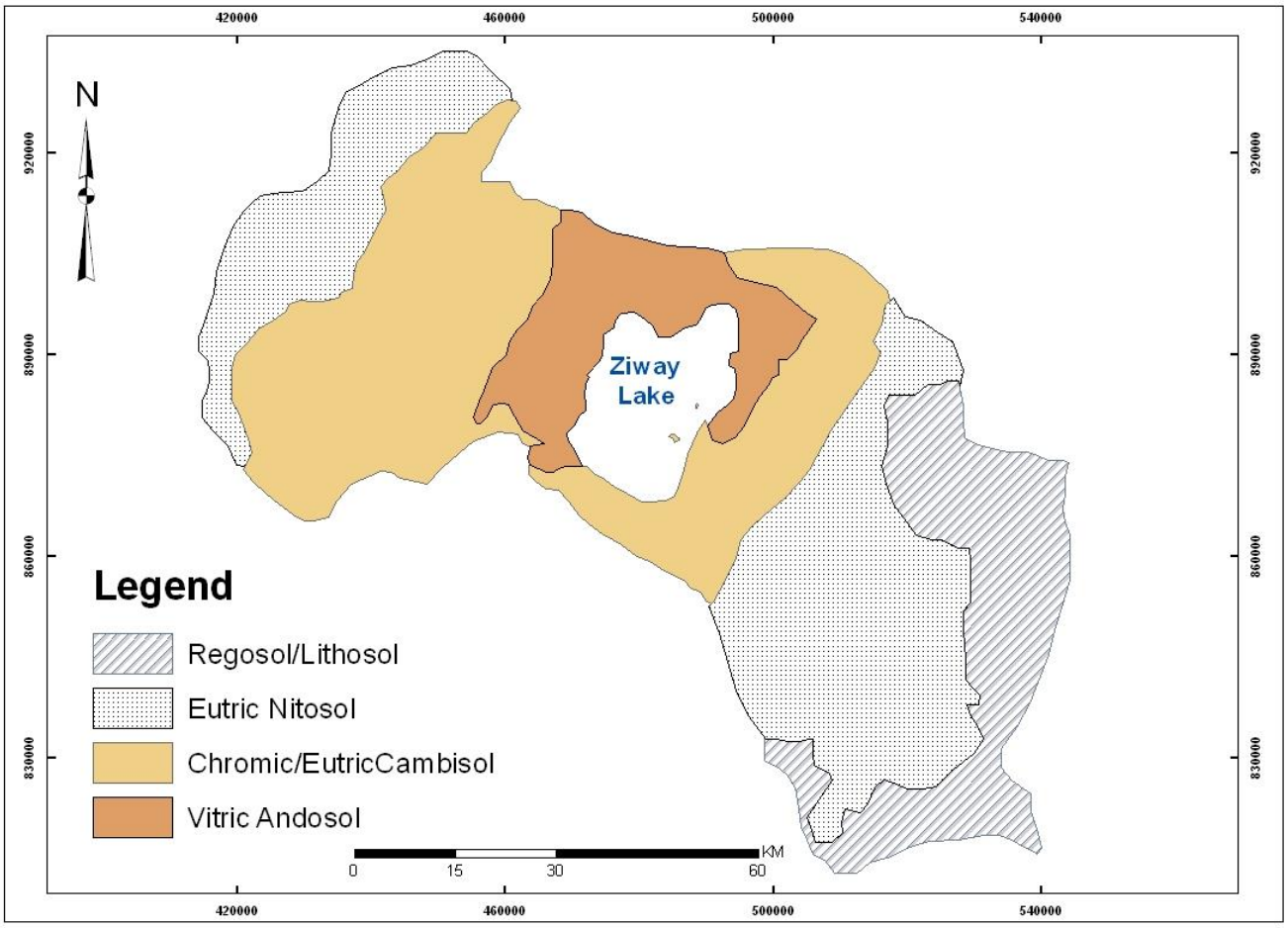

Source Makin (1976)

Figure 7 Soil map of the catchement

4. Geology

4.1. Regional Geology

Geological formation were deposited consist of different division rock unit which is related with land form, climatic condition, erosion and deposit forming history over geological time scale. Cenozoic volcano-tectonic and sedimentation processes that took place in the part of the eastern Africa and Ethiopia results geology and morphologic features and Early Mesozoic sediment accumulation over the Precambrian basement rocks is due to spreading of a shallow sea over much of Ethiopia as a result of land subsidence. Following the regression of the Mesozoic sea to the southeast a major uplift occurred, which is known as the Arabo-Ethiopian Swell. The upraised and up arched land mass fissuring under tension permitted the accentuations of voluminous basaltic magma to form the Ethiopian flood basalt province Mengesha Teferra et al (1996). This was followed by the development of full symmetrical grabens and rift-in-rift structures Di Paola (1972; Woldegabriel et al (1990), Le Turdu et al (1999) superimposed on the uplifted swell, part of the great East African Rift System started in the Miocene. The uplift, subsequent rifting and volcanism in the rift and outside the rift resulted into the formation of the present physiographic of Ethiopia. Large Volcano-tectonic collapse in the MER formed the Ziway-Shala basin.

Evolution of the Rift system is, lager subsidence of rift floor accomplished with shied volcanic in main Ethiopia Rift system. Crustal extension to the east gave rise to extinct Pliocene trachytic shield volcanoes including Chilalo, Galama and Kaka of eastern high land which rest on trap basalts Kunz et al (1975).

Acidic tuff, mostly ignimbrites are out cropped on the escarpment within Ethiopian rift then after the formation of escapement , fissural volcanism was confide to active Wonji fault belt running parallel to the rift axis Mohr (1967) .

4.2. Geological setting of the catchement

4.2.1 Nazareth group and Dino formation undifferentiated

9.5 – 3 million forming Nazareth group, mostly pantelleritic ignimbrites and lavas that were emitted from central formed along pre existing faulting parallel to the rift margin Gasparon, et al (1993).
Nazareth group is dominantly alkaline and alkaline stratoid, silicic, ignimbrites, unwellded tuff, ash, rhyolites and trachytes, with few meters thick.

Post Nazareth formation is Dino formation covers highlands, much of sloppy and the escarpment mostly cover with ignimbrites, tuff, pumice and pyroclastic deposits (figure 8).

4.2.2 Chilallo Volcanics

Rift volcanics, lava flow series i.e. post Miocene or Plio-Quaternary are an early alkaline silicic series followed by scoracious flood basalt intrusion which were post dated major rifting and faulting movement. Ryolites, trachytes, trachybasalt and alkali basalt outcropped in the eastern highland of Asela and Bekoji.

4.2.3 Basalts and associated flows of the rift floor

Pleistocene to Holocene, the formation includes basaltic hyaloclastites and recent basalts in the rift floor. The lava fields elongated parallel to main tectonic trend of the rift.
The basaltic groups are Wonji and Silte volcanics. The Wonji lava field lies on eastern escarpment with the thickness at about 100m and Butajra Silte area

4.2.4 The central rift volcanic complex

The variety of volcanic complex are formed the Ethiopia Rift. They are characterized by rhyolytic lava flows and domes associated with rift ignimbrites. In the area of Aluto, Gadamotta and Chobbi volcanoes alkaline and peralkaline silicic dominate composition outcropped. This group is divided in to three units with respect to the atudy area and descriped as follows

- are composed of silicic pyroclastic including pumice falls and ashes with subordinate lava flows . Aluto Volcanics are of late age Pleistocene-Holocene
- Bora-Bericho are formed in late Pleistocene-Holocene dominated with Silicic pyroclastic number of volcanics including Bora Volcano is found north of the catchment.
- Poorly welded pumice flows form Boricho volcanics which is found north east of Bora Volcano.
- Gadamotta Ryholite is composed of very thin alluvio-colluvial, volcaniclastic and fluvio-deltaic deposits resting erosively on older deposits through surface. On the Gademotta slopes the unit is represented by alluvial sands and gravels, overlain by alluvially reworked fine-grained greyish tuffs. In the Bulbula River Plain, 15–20 m thick subaerial pumice fall deposits, corresponding to the Abernosa Pumice Member, Street (1979).

4.2.5 Volcano- sedimentary rocks and lacustrine sediments

End of Pliocene to recent time interval sedimentary layering was carried. Identified litholostratigraphic unit were listed as follows

- Pelite dominated acustrine deposits: deposits of pelite and peat.
- Colluvium: Gravel,sand,silts and Volcanics pyroclastics (Mid Pleistocene-Recent)
- Alluvial deposit: Mainely terrace gravel,sand and silt associated locally with clay(Holocene- present).

- Deltaic and fluvial-deltic deposits: deposits of sand,siltandclay(Holocene)
- Meki and Kater deltic deposits:Sand,silt and clay(Holocene)
- Tufa fluvo-lacustrine deposit : Mainly gravel,sand,peliteand peat(Holocene)
- Ziway terrace and Volcano-lacustine deposits: Ash and tuff dominated pyroclatic formation with pelite,diatomite,silt and clay shore sand and shellbed
- Bulbula deposits: volcano-lacustrine deposits, mainely pyroclassstics derive from ashand tuff with subordinate shell beds.

4.3. Tectonic

The Ethiopia rift valley is NE- SW aligned, which runs for about 1000 Km and width 70 Km width Mohr (1971), Gasparon et al (1993). central main Ethiopia rift is Characterized by NE to NNE aligned structure forming parallel narrow faulting strips of land ,between two faulting down thrown land, rift valley structure , graben were formed .

Wonji fault belt an en-echelon stepping NS – NE trending faults, east of lake Ziway is observed in the catchement and affect the rift floor also (figure 8). East west extension indicated due to the pattern of step normal faulting structure of Boccalleti (1998).
Guraghe fault, western margin of the MER shows changes in trend at about 7 55 N. Eastern margin of MER also characterized by west dipping N 30 E – N40E trending border faults. I central part of MER the alignment of Volcanoes indicates presence of Extensional tectonics Teafaye Korma et al (1997).

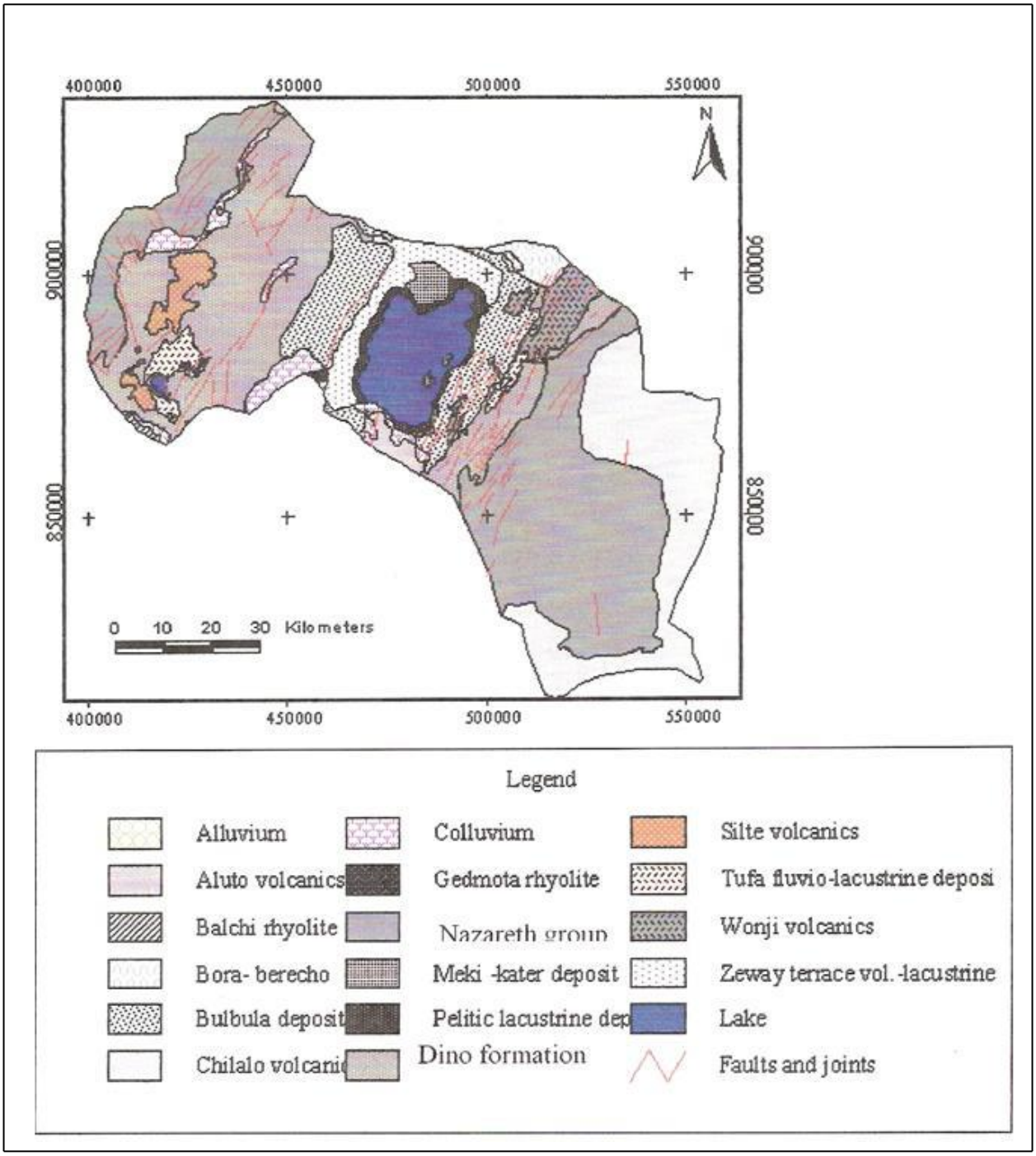

Source: Tenalem Ayenew(1998)

Figure 8 Geological Map

5. Hydrometeorology

In the study of water and environmental system related subject, understanding of hydrometerlogical characteristics (interrelation between atmospheric and land of hydrological cycle) is very important. Meteorological data are at various meteorological stations (figure 5) recorded are the basic inputs for studying the hydrometerlogical characteristics.

5.1. Precipitation

One of the major forms of precipitation received in the catchement is rainfall, it duration starts from June and ends in September which is the major rainy season for the catchment. Rainfall in the catchment is mostly governed by the position of the Inter Tropical Convergent Zone (ITCZ). ITCZ travel to north of Ethiopia, especially during peak rainy season of July to August. The dry season is lasting from October to February and also governed by shifting of the position of ITCZ to south of Ethiopia. During March to May small rain fall distribution occurs named as “Belg” season as in table 3, even though daily air temperature become peak.

Table 3 Point Precipitation Records From Meteorological Stations.

Station	Recording Periods	Jan	Feb	Mar	Apr	May	Jun	Jul	Aug	Sep	Oct	Nov	Dec	Annual
Abura	1967-1977	17	34	51	61	54	67	112	95	74	29	12	11	617
Arata	1974-2004	12	30	69	71	84	93	133	121	109	42	12	6	781
Asela	1966-2004	18	46	95	113	115	133	188	203	159	60	20	15	1167
Bokoji	1971-1999	25	51	87	104	102	108	177	187	87	58	15	12	1014
Bui	1970-2004	26	46	79	82	73	111	213	199	112	35	8	6	992
Butajira	1968-2004	38	67	136	127	115	125	173	172	116	45	11	14	1138
Digelu	1967-1977	31	50	71	91	91	108	175	179	84	52	24	21	976
Ejersalel	1967-2004	16	36	58	76	66	79	196	162	86	24	5	4	807
Kater Gunet	1987-2004	4	20	45	71	88	94	138	124	104	39	3	5	736
Kersa	1968-1997	26	47	78	104	95	78	113	122	106	57	21	11	858
Kosha	1974-2004	22	48	78	91	90	100	171	170	109	51	5	5	941
Kulumso	1966-2004	22	44	81	80	83	91	127	136	105	41	10	10	831
Meki	1965-2004	13	35	56	65	64	77	170	149	87	34	8	4	762
Meraro	1968-2004	36	41	71	105	87	98	179	185	92	46	23	20	983
Sagure	1973-2004	13	27	59	73	81	98	155	149	74	35	7	5	775
Torra	1974-2004	25	43	83	116	95	87	133	124	117	49		6	885
Ziway	1970-2004	17	30	56	75	72	83	14	122	86		2	4	732

5.2. Evapotranspiration

The term evapotranspiration are coupled process of evaporation and transpiration while these processes are not separately occurred due to the complex and heterogeneous environment.

Evaporation is the process in which liquid form of water is converted to water vapor and released into the atmosphere from the surface of evaporation taking place. Evaporation is occurring in open water body like lakes, rivers, wet vegetation, ponds and soil. Source of energy available to change the liquid water to vapor state are solar radiation, atmosphere and deep source of geothermal fields. The existing of water vapor pressure difference is an important factor for ET to occur between the evaporation surface and the atmosphere. Evaporation from soil surface occures when soil moisture is developed through frequent precipitation exist and irrigation activity is developed. Mostly soil has the nature of conducting water from beneath existing saturated portion to the surface. On later case also evaporation continued until moisture deficit is occurred.

Transpiration is also a process vaporization water from vegetation cover, where different cell structure, proportion of chlorophyll, water content and surface structure morphology of different plant have a marked effect on the process of transpiration to occur it is also the opening stomata aperture facilitate to take all water from leave surface but only few water is available in plant tissue.

Evapotranspiration can be explained over the growing period for growing crop as initially sowing period evaporation is taking from wet soil because degree of shading crop coverage almost considered 10%. When crop growing stage reaches at mid season transpiration takes the process of removal of water vaporization from canopy coverage increase over the top soil.

Factors affecting evapotranspiration

- Weather Elements are radiation, air temperature ,humidity and wind speed
- Crop characteristic include crop planting, rate of crop development and length of growing season.
- Management and environment aspect such as soil salinity, limited application of fertilizer

5.2.1 Air temperature

Atmospheric temperature which is recorded by four principal stations in the catchement as described in table 4, have influenced the rate of evapotranspiration by exerting sensible energy flux transfer when the temperature increased by solar radiation and atmospheric conversion release of long thermal radiation.

Table 4 Mean monthly temperature (Degree Celsius)

Station	Recording periods	Jan	Feb	Mar	Apr	May	Jun	Jul	Aug	Sep	Oct	Nov	Dec
Asela	1960-2004	14.3	15.6	15.9	16.4	16.5	15.8	14.9	14.7	15.9	14.9	14.1	14
Bui	1990-2004	16.6	17.3	18.4	18.6	19.5	17.5	16.2	16.3	16.7	16.4	15.8	15.7
Butajira	1972-2004	18.2	18.6	19.2	19.2	19.1	18.5	17.6	17.7	18.4	18.4	18.5	17.8
Kulumso	1966-2004	15.7	16.7	17.8	18.2	18.1	17.2	16.1	15.8	16	16.6	15.9	15.4
Meraro	1986-2004	14.3	14.9	15.8	15.9	16.1	15.2	14.5	14	14.2	14.7	14.1	13.5
Sagure	1981-2004	14	15.1	15.9	15.8	15.7	14.9	14.3	14.3	14.3	14.1	13.6	13.5
Ziway	1970-2004	19.3	20.4	21.4	21.5	21.8	21	19.9	19.7	19.9	19.7	18.9	18.7

5.2.2 Air humidity

The existing of water pressure different between surface and surrounding air causes evaporation to take place while an increase of air humidity decrease evaporation rate due to less water storing ability. In the catchment, water content of air expressed in relative humidity (RH) can be characterized by the following equation:

$$RH = 100\ e_a/e^o(T) \quad \text{.....Eq. (14)}$$

Where e_a is actual air vapor pressure and $e^o(T)$ is saturated water pressure.

Table 5 Mean monthly relative humidity (%)

Station	Recording periods	Jan	Feb	Mar	Apr	May	Jun	Jul	Aug	Sep	Oct	Nov	Dec
Bui	1990-2004	63	61	64	64	63	72	80	80	74	65	63	63
Kulumso	1971-2004	58	54	58	61	61	68	78	81	78	62	54	58
Meraro	1971-2004	62	57	58	69	67	73	82	82	78	73	65	62
Ziway	1970-2004	67	66	66	68	68	69	76	77	74	66	64	66

5.2.3 Wind speed

The extent of wind speed and air turbulence remove water vapor from the evaporating surface and has positive relation with evapotranspiration rate, four stations records are found in the basin as in Table 6.

Table 6 Monthly average wind speed records (m/s)

Station	Recording periods	Jan	Feb	Mar	Apr	May	Jun	Jul	Aug	Sep	Oct	Nov	Dec
Bui	1991-2004	2.1	2.1	2.1	1.8	2.1	1.6	1.5	1.4	1.4	1.9	2.1	2.1
Kulumso	1980-2004	2.6	2.5	2.2	2.1	2.2	1.9	2.1	1.7	1.3	2.7	3	2.8
Meraro	1991-2004	2.5	2.6	2.9	3	2.8	1.9	1.5	1.5	2	2.8	2.8	2.6
Ziway	1979-2004	1.4	1.4	1.3	1.3	1.5	1.9	1.8	1.6	1.1	1.2	1.5	1.5

5.2.4 Sun shine

Main source of energy supply is solar radiation in which weather station record as sunshine hourly as listed in table for long year records.

Table 7 Average sunshine hour (hour/day)

Station	Recording periods	Jan	Feb	Mar	Apr	May	Jun	Jul	Aug	Sep	Oct	Nov	Dec
Bui	1990-2004	8.9	8.4	8.2	8.1	8.2	6.8	5	5	6.8	8.7	9.9	9
Kulumso	1976-2004	8.1	7.8	7.3	6.7	7.2	7	5.3	5.3	5.6	7.5	8.7	8.7
Meraro	1989-2004	8.5	7.5	7.9	6.7	7.6	6.3	4.6	5.5	6.1	6.3	8.6	8.8
Ziway	1976-2004	9.5	9.4	8.3	8.4	9.2	8.4	6.4	6.6	7	9.1	10.2	10.1

Evaporatraspiration estimation using three approaches commonly proceeds as follows:

- Reference evapotranspiration which related for specific type of crop type, grass covered field,
- Crop coefficient Kc used to correct between the standard crop and the existing crop according to crop stage development, and assuming optimal amount of nutrition is available
- Actual evapotranspiration in which real existing situation of the features considered like stress is there, salinity problem.

ET can be also measured with field measurements. Most of field measurements are indirect and based on equations and assumsions. Lysimeters 1, the evapotranspiration for a given time period is determined by isolating the crop root zone from its environment and controlling the processes that are difficult to measure. As lysimeters are difficult and expensive to construct and as their operation and maintenance require special care, their use is limited to specific research purposes because it performance depend on precision of installation and that vegetation not hanging over the edge of Lysimeter.

Bowen ratio surface energy balance system depend on sensor accuracy to measure small difference in air humidity with tower installing instrument

$$\text{Bowen ratio} = H / ET \quad \text{Eq. (15)}$$

Where

H is sensible energy flux

Bowen ration result from equation result can compared with SEBAL but partitioning of H and ET is difficult.

Eddy correlation (standard) measures the wind speed with microphone setting on the instrument and also additional Meteorological elements are measured.

Scintillometers is an optical device used to record fluctuation in the refractive index of the turbulence atmosphere over the area.

Soil Moisture sensor is a classical method on which soil moisture is measured at the depth of two meter and one meter, but the problem is at more depth the percolation carried on.

Estimation of open water evapotranspiration using pan evaporation provides an index of meteorological elements on reference evapotranspiration. But Thornthwaite method used to determine evaporation using temperature as an index of energy available for surrounding environment to equate evaporation.

6. SEBAL Model

The Surface energy balance algorithm for land surface model (SEBAL) is used to evaluate using empirical relationship and physical measure approach Bastiaanssen et al (1998) to estimate actual evapotranspiration from mixed type of surface features cover. SEBAL procedure can be grouped into five main steps appropriate for automatic processing as displayed in figure 9. The preprocessing required for SEBAL on data inputs of the satellite spectral data are geometric correction including reprojection process, spatial frequency analysis for destripping and removal of cloud covered pixel value commenced at initial stage.

The over all ability of surface features to the reflected back radiation of all reflectance wavelengths (λ), Albedo (r_o) estimated as in Zhong and Li (1988).
Normalized difference vegetation indices (NDVI) over 0.62- 0.67 (red band) and 0.841-0.846 (near infrared band) optical sensed by MODIS Terra product used. Emissivity (ε_o), a measure of natural materials as the ratio between its radiation emittance for a particular wavelength at a given temperature and that of a black body is estimated based on NDVI according to Moran and Jackson (1991).

Residual of the energy balance method which uses the three major components of energy partitions are known then actual ET equated as equation 16, indirectly.

$$Rn = G_o + H + \lambda_{ET} \quad \text{.....Eq. (16)}$$

Where
Rn is net radiation ($w.m^{-2}$),
G_o the Soil lost to soil ($w.m^{-2}$)
H the heat lost to atmosphere ($w.m^{-2}$) and
λ_{ET} the latent heat of vaporization ($w.m^{-2}$)

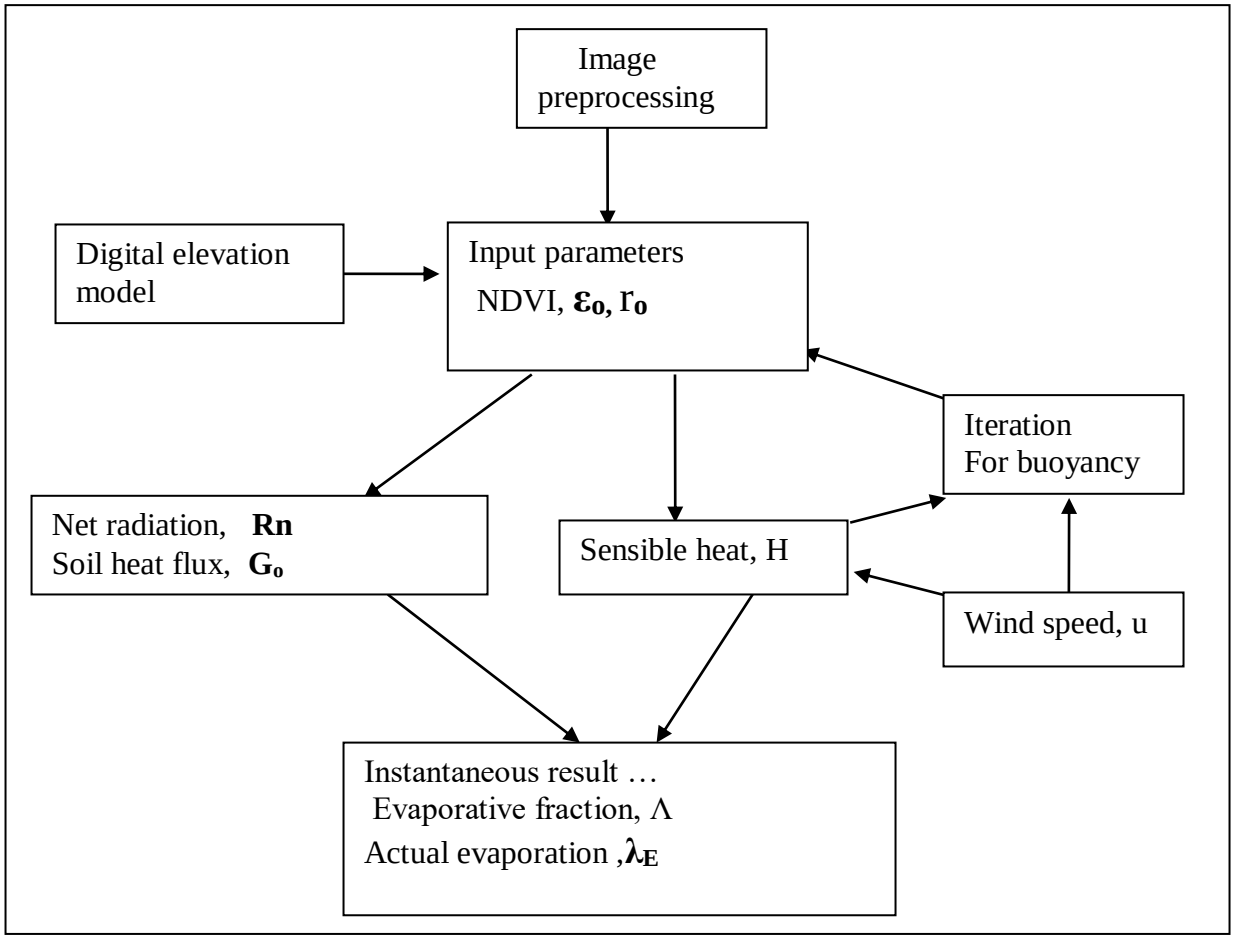

Figure 9 SEBAL Flow chart.

The net available radiation energy is equated from various component of radiation as discussed section 1.6. Extraterrestrial radiation received solar radiation at the top of earth atmosphere is uniform but vary on surface due to day time angle between ray of sun and earth surface which was corrected with atmospheric transmissivity as equation 2.

The net available radiation have different time scale during satellite over pass up to periods elapsed between consecutive satellite over detecting so exterritorial radiation changes because position of the sun ,lengths of the day vary hence it become the function of latitude ,date and time of day (FAO irrigation paper No. 56 irrigation book).

Computation of soil heat transfer across the layer is a function of the gradient of temperature between the surface and the soil layer it also depend on the thermal inertia of the soil. Instantaneous soil flux mostly have small fraction (figure 10) then it become zero if daily time is calculated due to day time stored energy will lose then after. since the remote sensing technique unable to detect at depth an empirical studies developed by de Bruin and Holtslag (1982) showed that the ratio G/Rn is related to the amount of vegetation present Jackson et al (1987) and Kustas and Daughtry (1990) developed empirical relations (Equation 17) between the ratio G/Rn and the normalised difference vegetation index (NDVI) .

$$G_o / Rn = (0.00075 * T_s - 0.05) * (1 - NDVI^4) \quad \text{Eq. (17)}$$

The Sensible heat flux is computed with SEBAL model by iteration process to describe the buoyancy effect on the aerodynamic resistance of the land surface (r_{ah}).

The temperature different between land surface and the air is scaled over the image required to match the range of sensible heat in a given turbulence condition obtained for the two extreme dry and wet pixels. Standard Monin-Obukhov theorem for turbulence exchange process as in equation 18 is followed by SEBAL approach to estimate H.

$$H = \rho_a c_p T^* u \quad \text{Eq.(18)}$$

Where

ρ_a ($kg.m^{-3}$) = the air density of moist air

c_p (J/kg/k) = specific heat at constant pressure

T (K) = the temperature scale

U (m/s) = friction velocity

water body surface were selected as cool pixels assumed to be wet than land features where sensible heat transfer is zero and driest pixel at rift floor identified with negligible evapotranspiration manually taken from thermal infrared band image. The temperature different between land surface and the air is scaled over the image by a linear relation with two anchor wet and dry pixel values.

Concept of evaporation fraction (Λ) is a key parameter in SEBAL model as express in equation 20.

$$\Lambda = \lambda E / \lambda E + H \quad \text{Eq. (19)}$$

$$\Lambda = \lambda E / Rn - Go \quad \text{Eq. (20)}$$

If $\Lambda = 1$ mean that $\Lambda = \lambda E$ where H goes to zero

And

$\Lambda = 0$ mean $\lambda E = 0$ where no available energy is for evaporation.

And

$\Lambda > 1$ is only if $H < 0$ during sensible heat is negative when heat absorbed from air especial at day time around the lake in case of Ziway

Following Brutsaert and Sugita, 1992; Crago, the instantaneous evaporative fraction is considered similar to its daily counterpart and is

- Used to compute the actual 24-hour evaporation from the instantaneous latent heat fluxes as equation 21.
- To crop parameters would be useful for monitoring of biomass and prediction of grain as equation 11.

Evapotranspiration is calculated as the instantaneous evaporative fraction times the daily net radiation as follows

$$ET\ daily = \Lambda * Rn\ daily \quad \text{Eq. (21)}$$

When assessing the effect of solar radiation on evapotranspiration, one should also bear in mind that not all available energy is used to vaporize water. Part of the solar energy is used to heat up the atmosphere and the soil profile as indicated in figure 10.

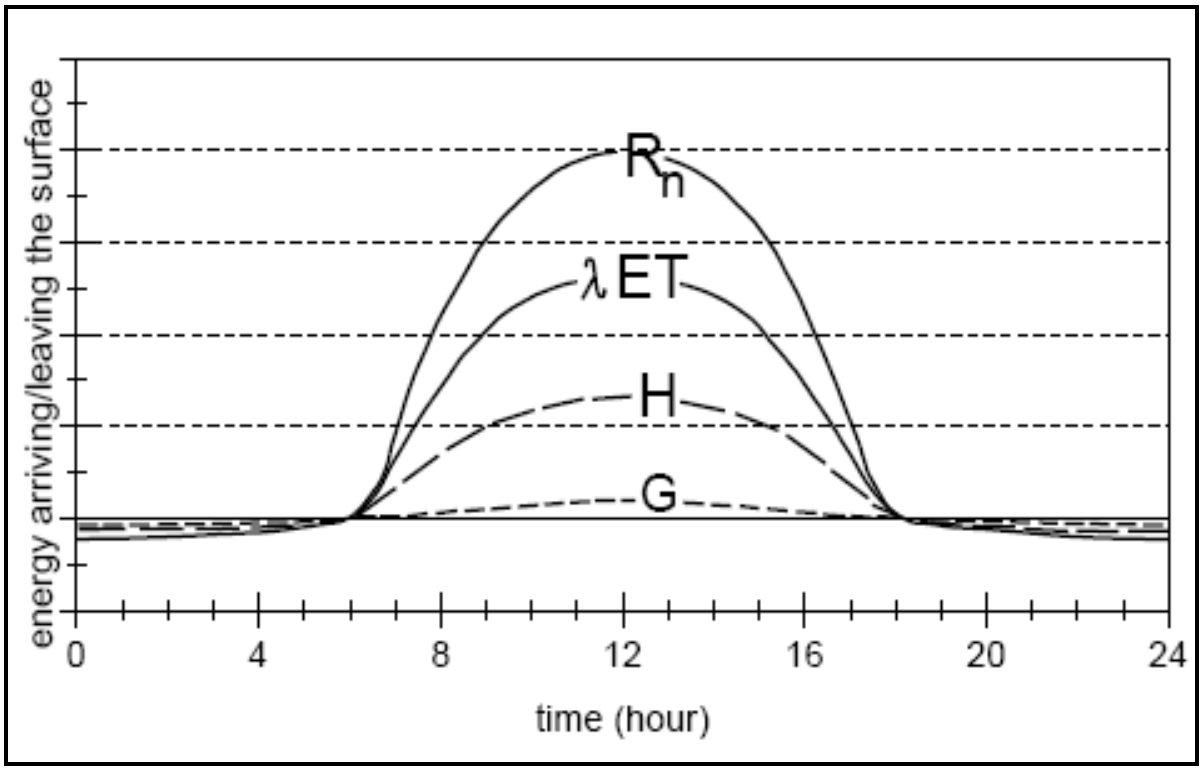

Figure 10 Schematic presentation of the diurnal variation of the components of the energy balance above a well-watered transpiring surface on a cloudless day.

Projection of daily evapotranspiration to periods values (weeks or months), SEBAL uses the assumption of ratio of actual evaporation to the reference evaporation is constant to the ratio of actual evaporation to monthly reference evaporation. Morse et al (2000), Allen et al. (2001).

Ea/Eo (daily) = Ea/Eo (monthly)…… Eq. (22)

Where Ea daily is computed from SEBAL model

Eo daily and monthly is computed by FAO penman-Monteith method is recommended as the sole standard method with in form of the combination in equation 23.

$$\lambda_E = \frac{\Delta(Rn - G) + \rho_a c_p (e_s - e_a)/ r_a}{\Delta + Y (1 + r_s/r_a)} \quad \text{..... Eq. (23)}$$

Where: Rn is the net radiation,

G is the soil heat flux,

(e_s-e_a) represent the vapor pressure deficit of the air,

ρ_a is the mean air density at constant pressure,

c_p is the specific heat of the air, Δ represent the slope of the saturation vapor pressure temperature relationship , Y is the psychrometric constant and r_s and r_a are the bulk surface and aerodynamic resistance.

Reference evapotranspiration used for reference crop with required green cover and well wetted assumption. It is on specific land cover which is grass and also required meteorological data as formulated at equation 23.

6.1. Validation of SEBAL model

Validation for a model of SEBAL using remote sensing technique at catchments and field scale examined of the accuracy with existing field measured methods at different environmental conditions according to Bastiannssen (2005) as shown in Table 8.

Table 8: SEBAL model validation with different convectional techniques.

Field instrument	country	Location and year	Landscape	No of image Compared	source	Deviation instantaneous	Deviation 1- 10 days (%)
Drainage Lysimeter	US	Montpellier, Indaho,1989	Irrigated native sedge forage	4	Morse et al. (2000) Allen et al (2002)	NA	16
Weighing Lysimeter	US	Kimberly, Indaho, 1989	Irrigated sugar beet	12	Trezza(2002) Tasumi(2003 Allen et al (2002)	NA	20
Bowen ratio	Egypt	Qattara Deoression,1986	Playas and desert surfaces	3	Bastiaanssen and Menenti (1990)	NA	2
Bowen ratio	Spain	Tomelloso,1991	Rain fed crops	4	Pelgrum and Bastiaanssen	17	NA
Bowen ratio	Kenya	Naivasha,1998	Savannah	10	Fara(2001)	NA	16
Bowen ratio	France	Alpilles,1996	Alfafa,wheat sun flower	55	Jacob etal (2002)	3[a]	NA
Eddy correlation	Spain	Tomelloso,1991	Rainfed and irrigation	6	Pelgrum and Bastiaanssen	33	NA
Eddy correlation	Chine	Zhangye, 1991	Irrigated maize and desert	2	Wang et al ,(1995)	9	NA
Eddy correlation	Niger	Niamey,1992	Savannah, tiger bush ,forest	3	Roerink,1995	10	NA
Eddy correlation	The Netherlands	Cabauw Garderen,1995	Forest, pastures	11	Bastiaanssen and Roozekran,2003	NA	30
Scintillometer	Morocco	Marrakech,2003	Olive	17	Van den Kroonenberg A. (2003)	16(NOAA)	NA
Scintillometer	France	Alpilles,1997	Sunflower, Wheat, bare soil	1	Lagouarde et al.(2002)	1[a]	NA
Scintillometer	Botswana	Maun,2001	Savannah	1	Timmermans etal. (2003)	1[a] 100	NA
Average						14%	15%

Note NA = Not applicable, a validation at sensible heat flux

7. Result and discussion

Actual evapotranspiration maps were prepared over the entire Ziway catchment. Daily evapotranspiration were integrated from the evaporation fraction results made on year 2004 imageries which are radiometric and geometrically corrected to the SEBAL model application with discarding of some cloud covered imageries. The actual evapotranspiration for January 1st,February 9th,March 22th,May 20th, June 8th,July 1st, October 19th , November 25th and December 4th illustrated (figure11) the spatial variability of evapotranspiration over the catchement.

The daily evapotranspiration results ranging from 0.5 up to 8.5 mm/day .In the rift floor, actual evapotranspiration rate estimated 0.5 to 1.7 mm/day in the area where rain fall deficit measured and on the intensively traditionally cultivation farm lands when it was left uncultivated causes to posses less soil moisture content. Relatively high values 3.6- 5 mm/day were estimated on area where acacia woodland mixed with dispersed semi ever green bush and with spread irrigation schemes exist on swampy area .

High variable actual ET in the catchment occurred due to changes in geology, topography, rainfall distribution and land cover. In some of the highlands including Butajira areas , follows east facing slope aspect in which more solar radiation absorbed and due to rainfall distribution with vegetation coverage of the area, quite high actual ET and there is zonation with altitude related effect were observed.

However, evapotranspiration estimated from lake Ziway demonstrate that relative spatial difference of evapotranspiration derived as shown in figure 11. Larger portion of the lake estimated around 7.5 mm/day where maximum depth is found. When you swim to the lake shore the evaporation value is decreases on average up to 5 mm/day. The variation of actual ET over the lake also approved that it is a function of alebdo and emissivity of the lake body rather than temperature only. Therefore, the interaction of solar energy with the Lake depend on the reflectance property of the lake with considering the presence of suspended sediments which increase the bouncing of coming radiation from being absorbed as shown in plate 2, on which high green coverage and other activities carried at most edge of the lake. Moreover, at the confluence of Meki and Ketar rivers into lake Ziway the actual evapotranspiration is decreased. This can be related with large quantity of water flowing to the north and northeast part of the Lake.

Actual evapotranspiration 2.6 – 4.7 mm/day were also estimated on eastern and western highlands covered with mixed crops, grazing land and dispersed trees with the average annual rainfall about 1150mm. At the top of large volcanic peaks up to 8.5 mm/day of high actual evapotranspiration rate retrieved. This is because forest coverage transpired more water than cultivated farm land in the rift floor through intercepting water at high rate due to the rough surface resistant assist the rate of transpiration ,in addition forest root system are deep rooted can use more soil moisture and water saturated zone in dry condition to maintained their optimum temperature balance. Figure 11 displayed daily actual evapotranspiration of the different land use and land cover types over the images indicated that the spatiotemporal variation regardless of uneven distribution of cloud on satellite images reduce/enhance the value of actual evapotranspiration.

Plate 2 Lake shore (Ziway).

(a)

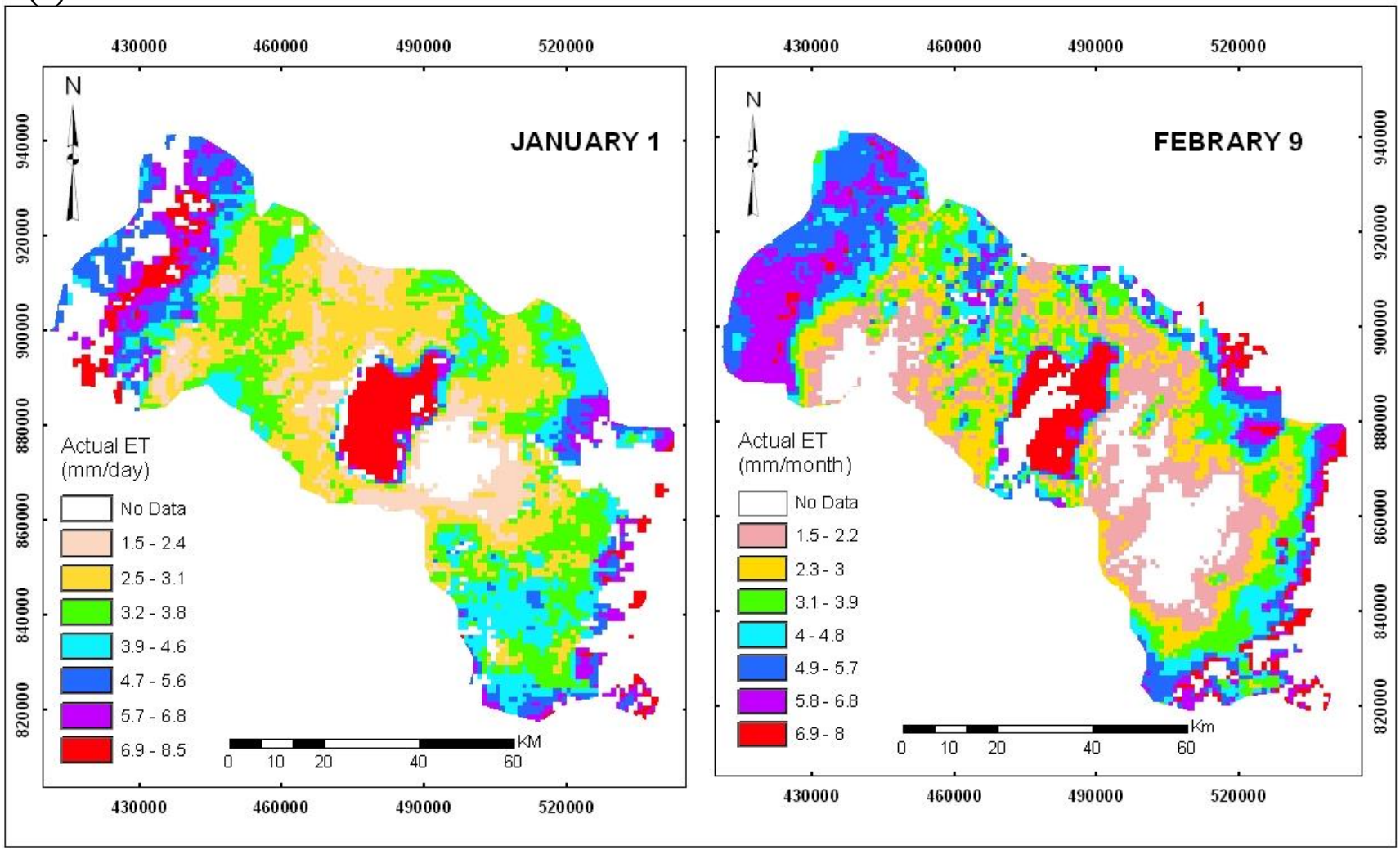
430000
460000
490000
520000
940000
920000
900000
880000
860000
840000
820000
N
JANUARY 1
Actual ET
(mm/day)
No Data
1.5 - 2.4
2.5 - 3.1
3.2 - 3.8
3.9 - 4.6
4.7 - 5.6
5.7 - 6.8
6.9 - 8.5
KM
0 10 20 40 60
FEBRARY 9
Actual ET
(mm/month)
No Data
1.5 - 2.2
2.3 - 3
3.1 - 3.9
4 - 4.8
4.9 - 5.7
5.8 - 6.8
6.9 - 8
Km
0 10 20 40 60

(b)

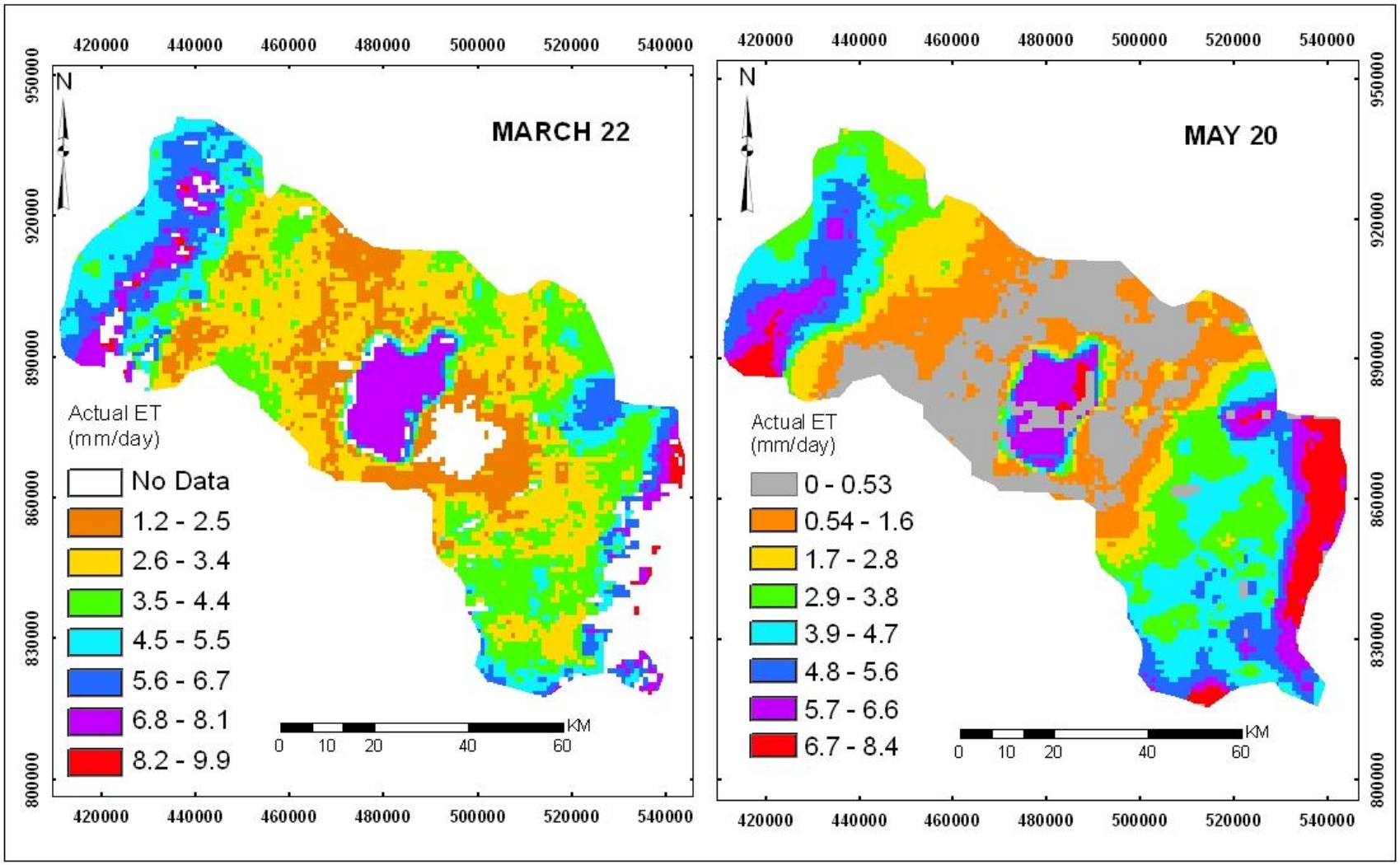
420000
440000
460000
480000
500000
520000
540000
950000
920000
890000
860000
830000
800000
N
MARCH 22
Actual ET
(mm/day)
No Data
1.2 - 2.5
2.6 - 3.4
3.5 - 4.4
4.5 - 5.5
5.6 - 6.7
6.8 - 8.1
8.2 - 9.9
0 10 20 40 60
KM
MAY 20
Actual ET
(mm/day)
0 - 0.53
0.54 - 1.6
1.7 - 2.8
2.9 - 3.8
3.9 - 4.7
4.8 - 5.6
5.7 - 6.6
6.7 - 8.4

(c)

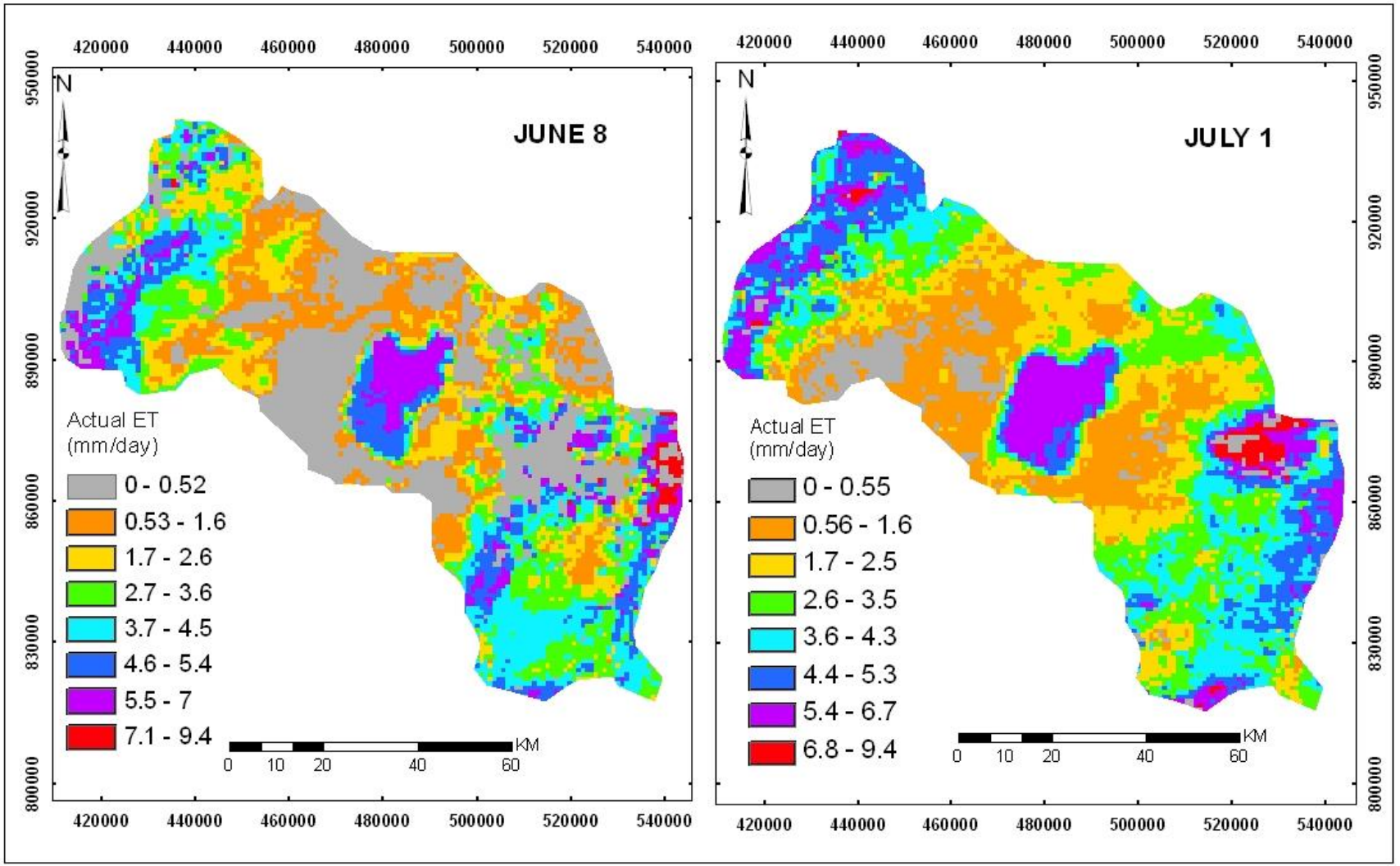
JUNE 8
N
Actual ET
(mm/day)
0 - 0.52
0.53 - 1.6
1.7 - 2.6
2.7 - 3.6
3.7 - 4.5
4.6 - 5.4
5.5 - 7
7.1 - 9.4
KM
0 10 20 40 60
JULY 1
N
Actual ET
(mm/day)
0 - 0.55
0.56 - 1.6
1.7 - 2.5
2.6 - 3.5
3.6 - 4.3
4.4 - 5.3
5.4 - 6.7
6.8 - 9.4
KM
0 10 20 40 60
420000 440000 460000 480000 500000 520000 540000
950000 920000 890000 860000 830000 800000

(d)

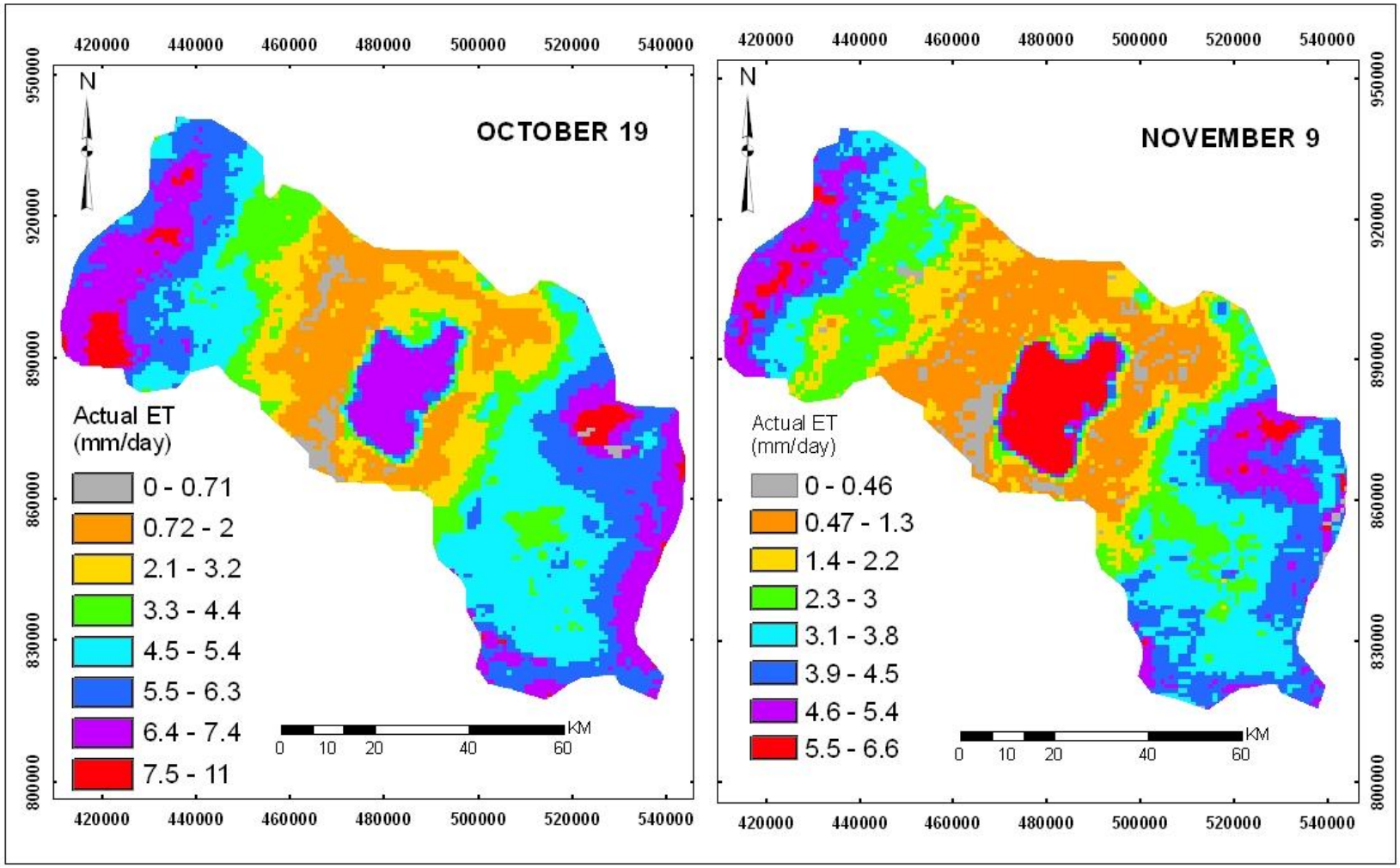
OCTOBER 19
N
Actual ET
(mm/day)
0 - 0.71
0.72 - 2
2.1 - 3.2
3.3 - 4.4
4.5 - 5.4
5.5 - 6.3
6.4 - 7.4
7.5 - 11
0 10 20 40 60 KM
NOVEMBER 9
N
Actual ET
(mm/day)
0 - 0.46
0.47 - 1.3
1.4 - 2.2
2.3 - 3
3.1 - 3.8
3.9 - 4.5
4.6 - 5.4
5.5 - 6.6
0 10 20 40 60 KM
420000 440000 460000 480000 500000 520000 540000
950000 920000 890000 860000 830000 800000

.

(e)

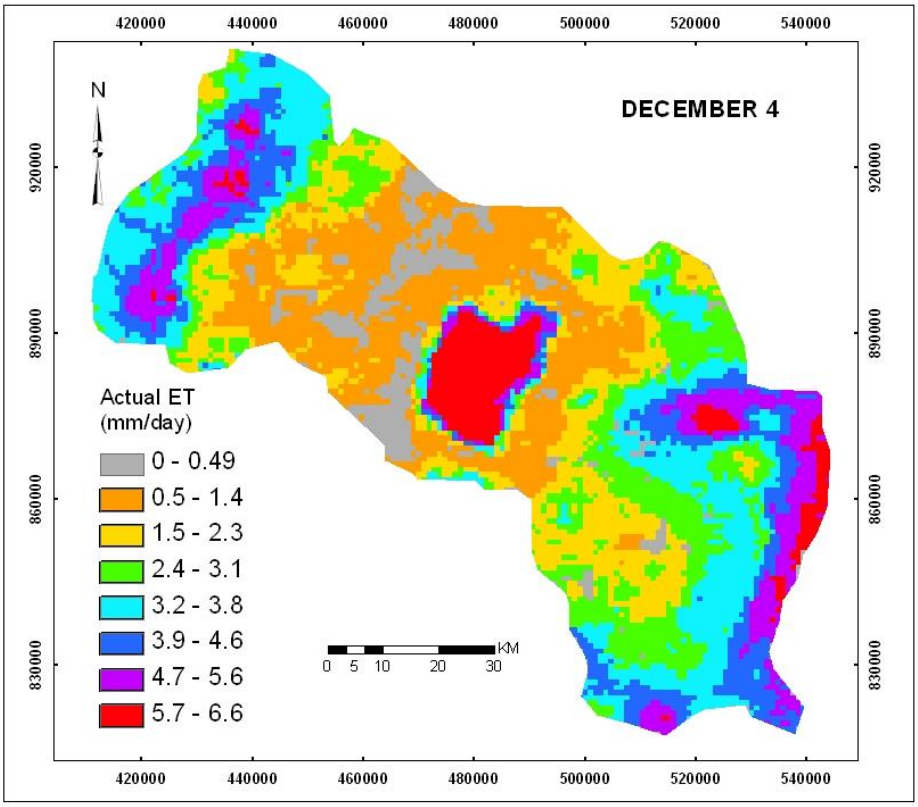

Figure 11 Estimated daily actual evapotranspiration in mm/day above (a-e) for 2004

Computing of monthly actual evapotranspiration from the daily actual evapotranspiration, were derived using equation 22 as shown in figure 12.The maps display the temporal variation of actual evapotranspiration observed over the series of imageries with frequency distribution graphs. Relatively lower actual ET less than 40 mm/months were estimated on the rift floor and adjacent highlands during the rainy season (June to July) due to the presence of high humidity.

During the dry months October- November, less than 70 mm/months of actual ET were estimated on large area coverage of traditional cultivated farm lands but actual ET was reached highest on wetland up to 132 mm/month. The uneven rainfall distribution effect were reflected on actual ET to increase in the lower region estimated 40-96 mm in January.

Open woodland covering the highlands and escarpment shows slight variation of actual ET about 130mm/month in rainy season and 160mm/month in dry period. Figure 12 below shows monthly actual ET seasonal variation with its histogram distribution.

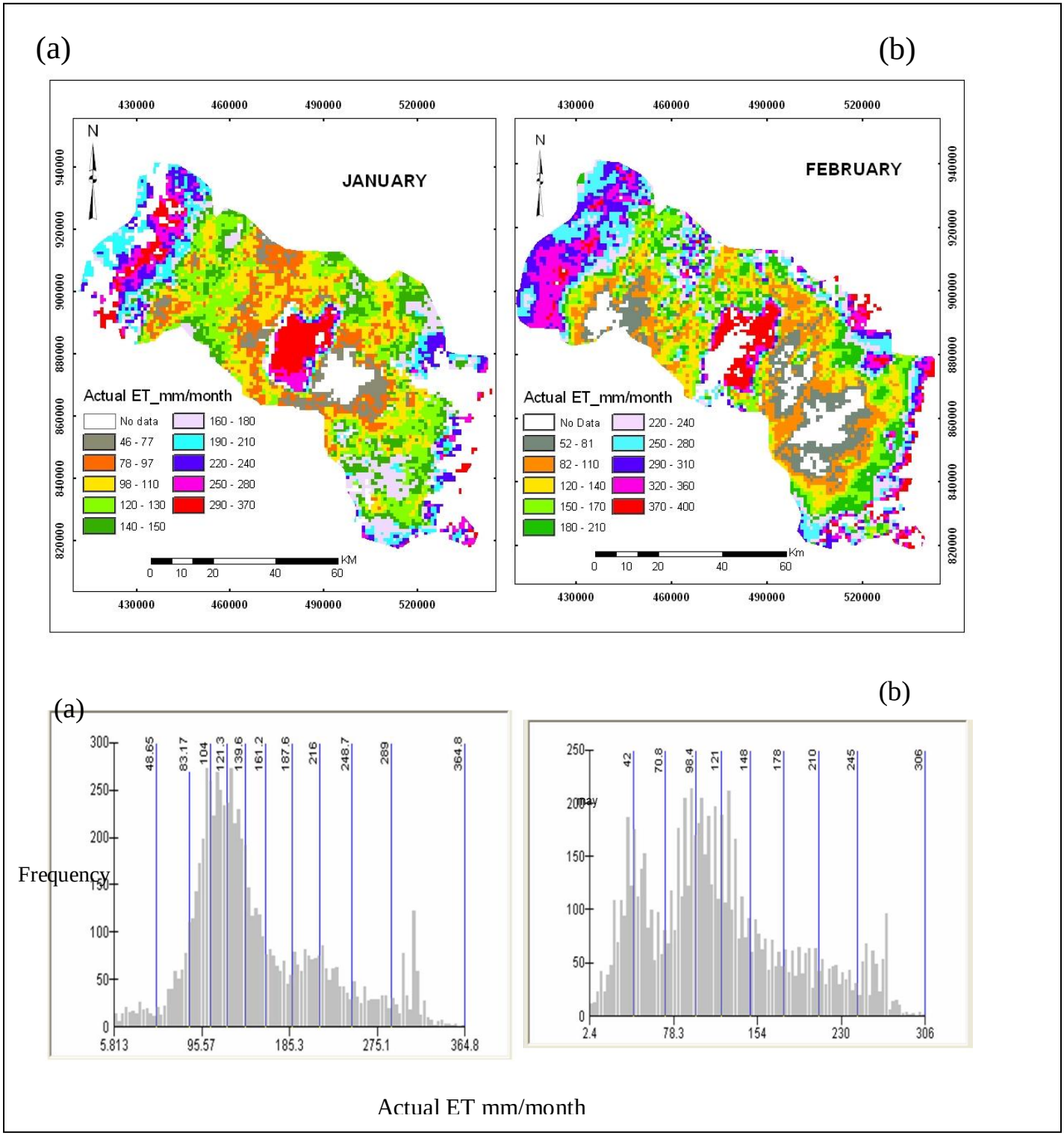

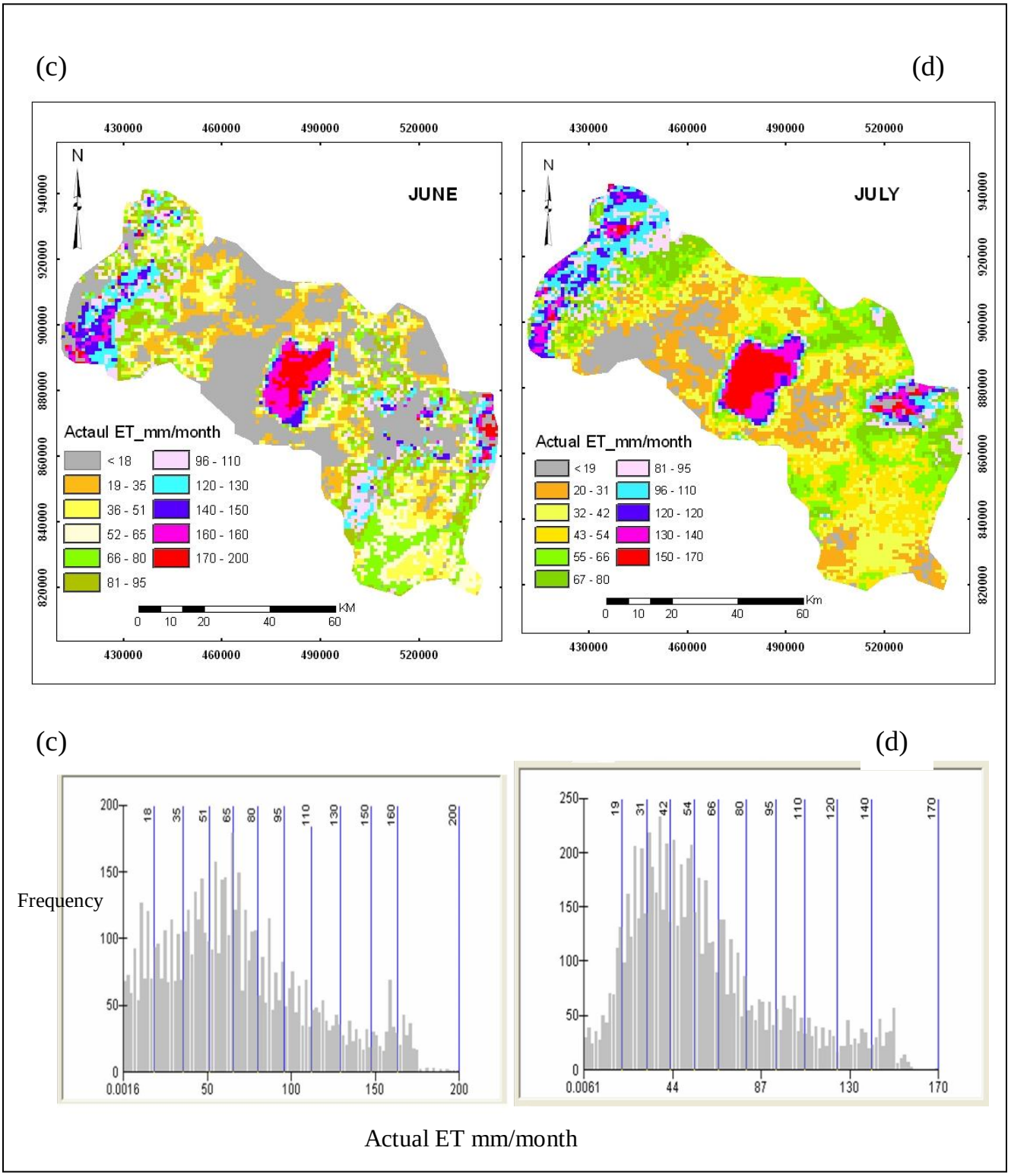
(c)
(d)
JUNE
JULY
N
Actaul ET_mm/month
< 18
19 - 35
36 - 51
52 - 65
66 - 80
81 - 95
96 - 110
120 - 130
140 - 150
160 - 160
170 - 200
Actual ET_mm/month
< 19
20 - 31
32 - 42
43 - 54
55 - 66
67 - 80
81 - 95
96 - 110
120 - 120
130 - 140
150 - 170
KM
Km
0 10 20 40 60
430000 460000 490000 520000
820000 840000 860000 880000 900000 920000 940000
(c)
(d)
Frequency
0.0016
0.0061
Actual ET mm/month

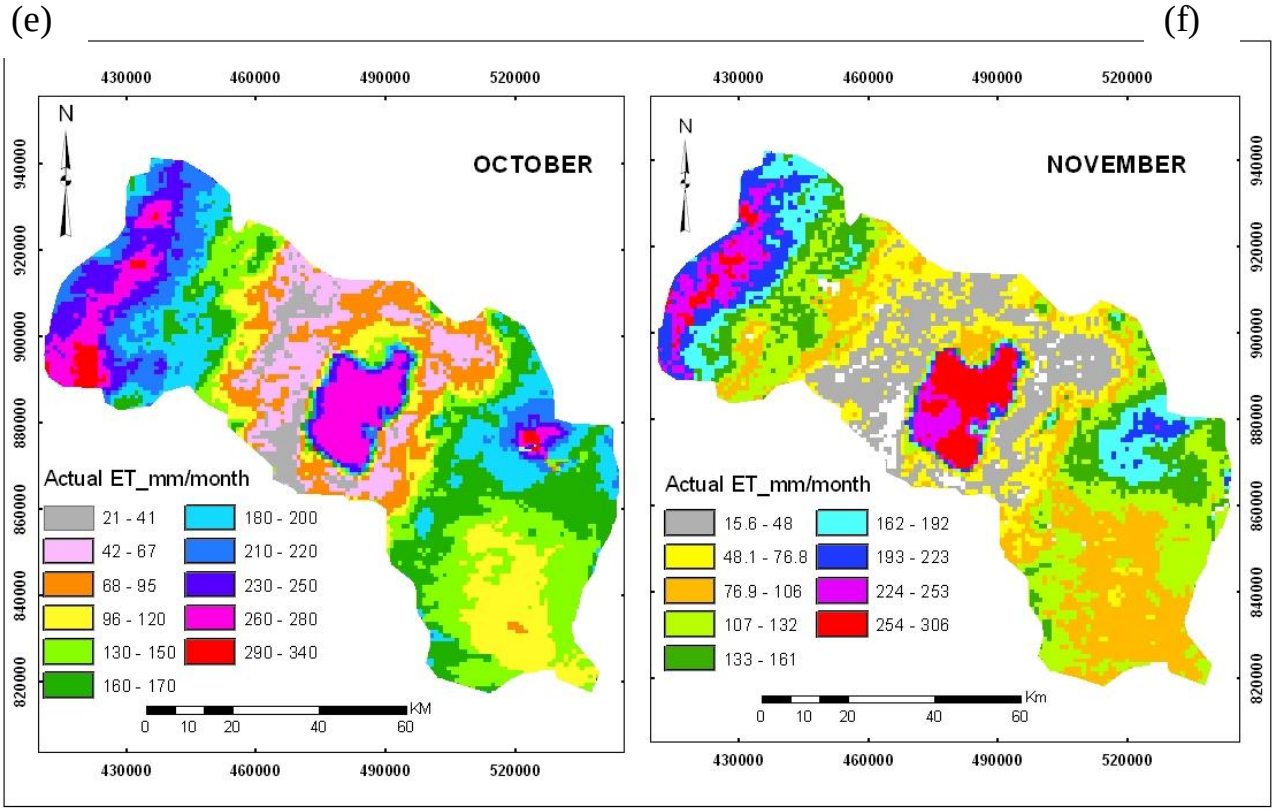
(e)
(f)
OCTOBER
NOVEMBER
N
Actual ET_mm/month
21 - 41
42 - 67
68 - 95
96 - 120
130 - 150
160 - 170
180 - 200
210 - 220
230 - 250
260 - 280
290 - 340
15.6 - 48
48.1 - 76.8
76.9 - 106
107 - 132
133 - 161
162 - 192
193 - 223
224 - 253
254 - 306
KM
Km
0 10 20 40 60
430000 460000 490000 520000
820000 840000 860000 880000 900000 920000 940000

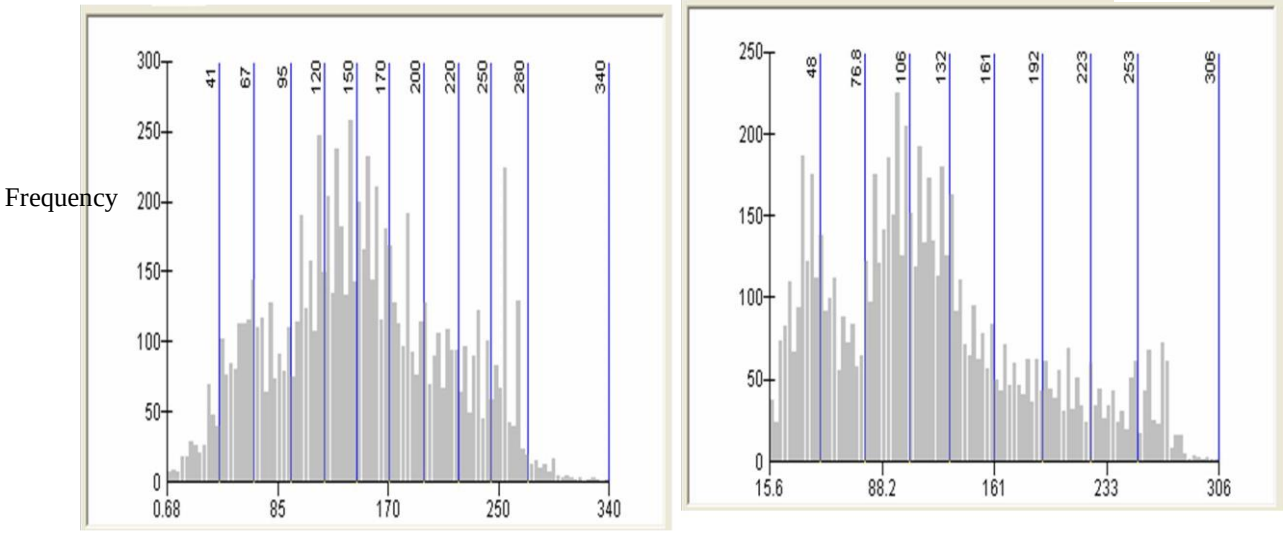
(e)
(f)
Frequency
41 67 95 120 150 170 200 220 250 280 340
0.68 85 170 250 340
48 76.8 106 132 161 192 223 253 306
15.6 88.2 161 233 306
Actual ET mm/month

(g)

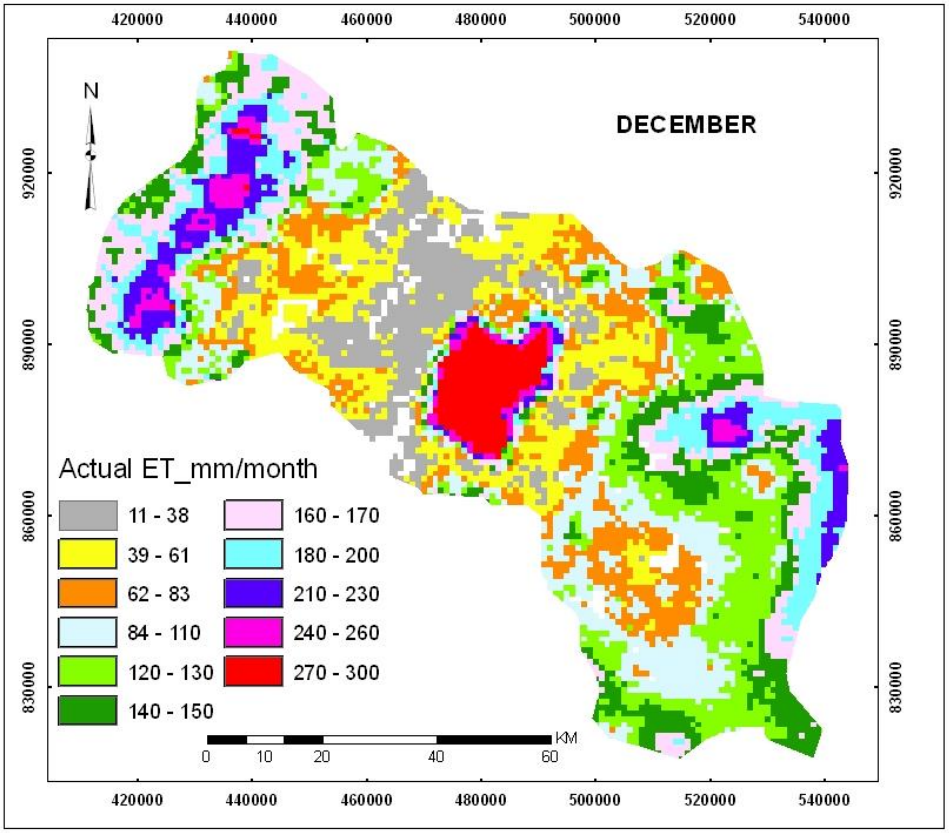

(g)

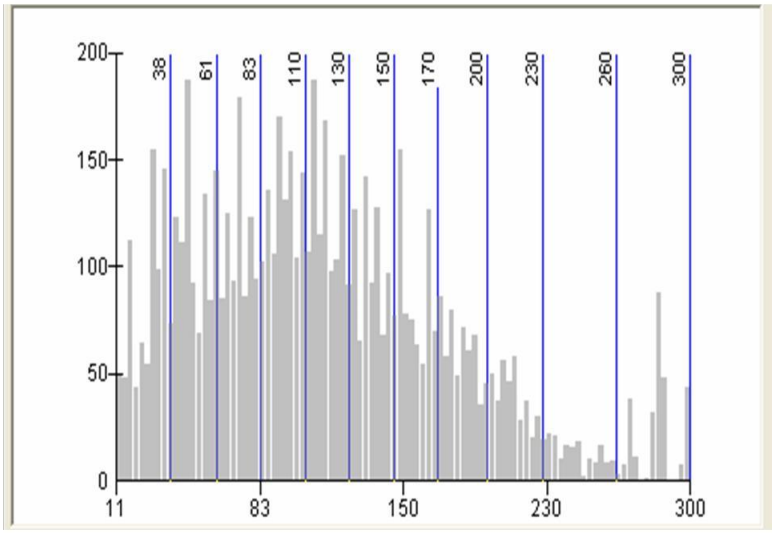

Figure 12 Monthly evapotranspiration (a-g) imageries and Histograms of 2004.

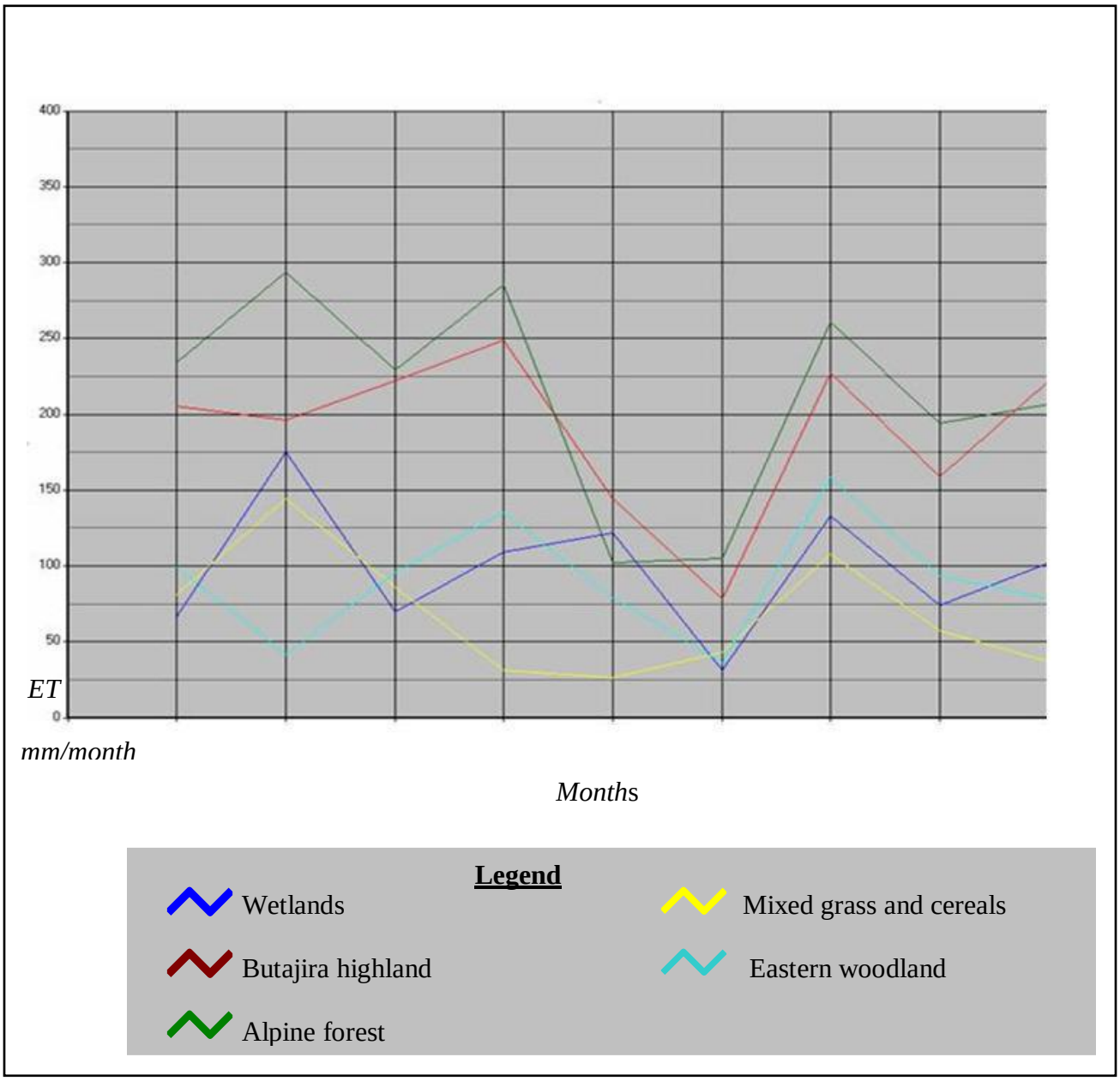

Figure 13 Monthly Actual Evapotranspiration at Selected location over the imagies (1: January, 2: February, 3: March, 4: May, 5: June 6: July 7: October, 8: November, 9: December)

The results as shown in figure 13, in rainy season June-July Actual ET over land uses decreases but in dry season the values reaches maximum. While in wetted lands mostly around the lake region actual ET looks similar except in rainy season became decreased. However, higher and constant values of actual ET were estimated over densely forest covered areas.

Comparison between SEBAL monthly actual evapotranspiration results with long-term evaluation of average actual evapotranspiration with Thornwaite and Penman (Annex 5-6) found that SEBAL result were greater than Thornwaite and Penman. The difference between conventional methods and SEBAL result most probably explained as Thornwaite assume that air temperature has contribute much to evaporation process but SEBAL considered albedo, surface temperature and emmisivity of the features contribute to the evapotranspiration process. It is also notice that penman uses only weather data with insitu physical measurements data like soil moisture.

Computing of average monthly dry biomass production from NDVI (figure 16), evaporation fraction from SEBAL and active photosynthesis radiation (Figure 15) using equation 9 were derived in summer season over intensively cultivation activity in rift floor around the flat land. Figure16 and figure17 showed that the potential of biomass production variation demonstrated through the crop growing period at different stage as listed below:

- Crop Development stage ; Surface cover 70-80% cover at July 2005
- Mid-season stage; effective full ground cover and start of maturity at August 2005 and September 2005 respectively.
- Late season stage; end maturity stage or harvesting, at October 2005.

Spatial distribution of biomass production in figure 17a displayed that single peak bar graph exists which indicates, majority part of area were covered with less dry biomass since the period was at stage of crop development. While on August unimodal type of histogram with wide width exists, indicates that biomass production increased up to 150 Kg/ha and biomass heterogeneity was observed. Eventually shifting of the graph to the right side with narrow width indicates that higher and less contrasts of biomass were observed on the month of September. Where as, gradual decline in biomass production on same area was derived during harvesting crops stage. On highlands high values of biomass reserved up to 200Kg/ha this due to the crops grown dominantly are C3 type. As with Annex 2 average biomass production derived for standard crops was compared with this study results found that they have small variation due to incoming short radiation (figure 15).

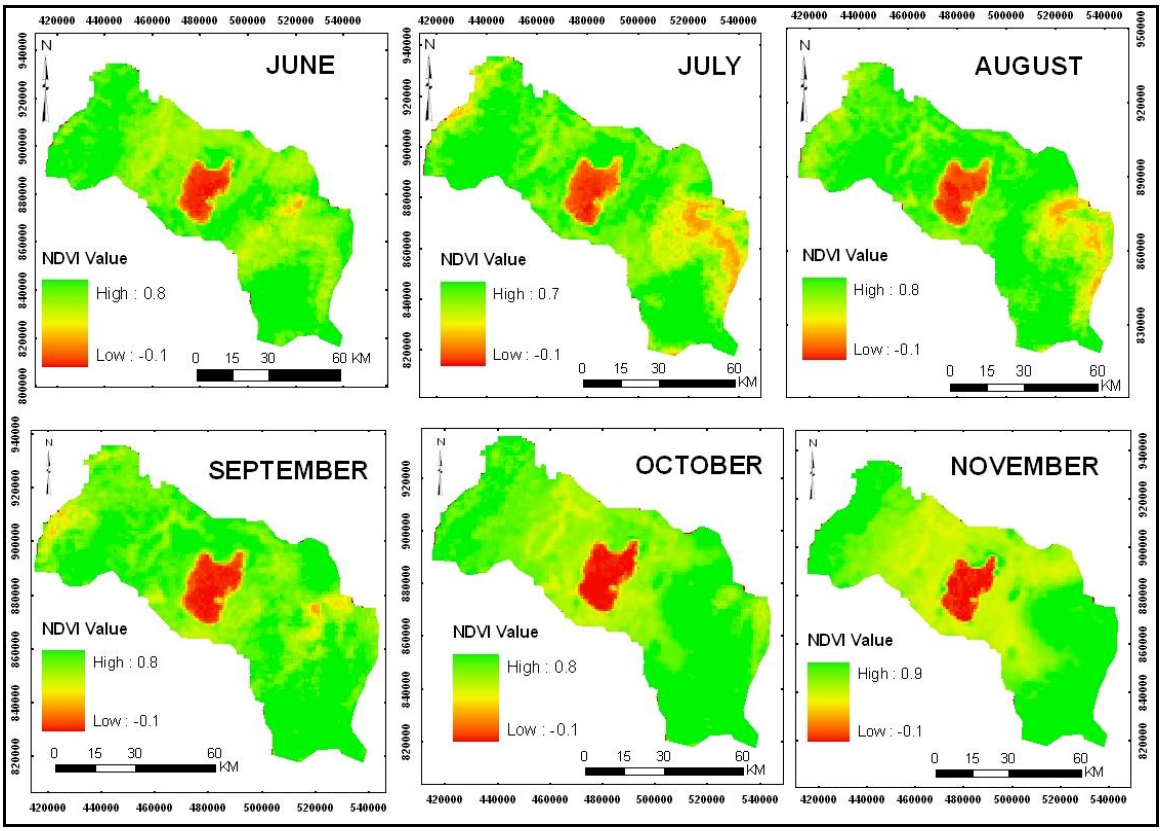

Figure 14 Normalized difference vegetation index series images of 2005 year of months from spot vegetation.

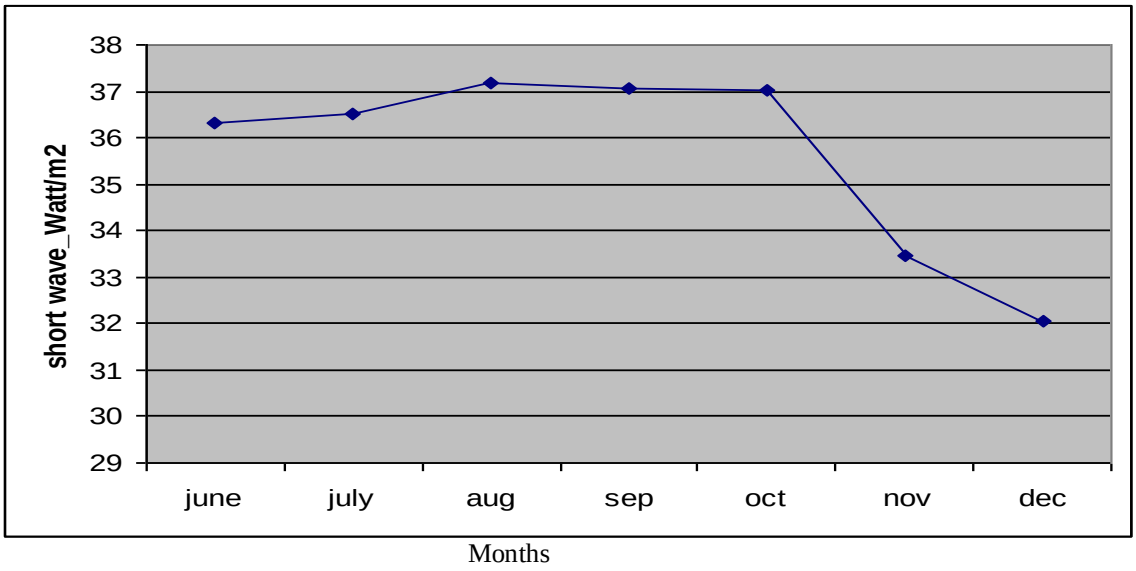

Figure 15 Incoming short wave radiation: 2005

Figure 17 demonstrates potential dry biomass production over summer season in which crop requirement of water, nutrition, fertilizer are assumed sufficient that do not affect crop growth potential production.

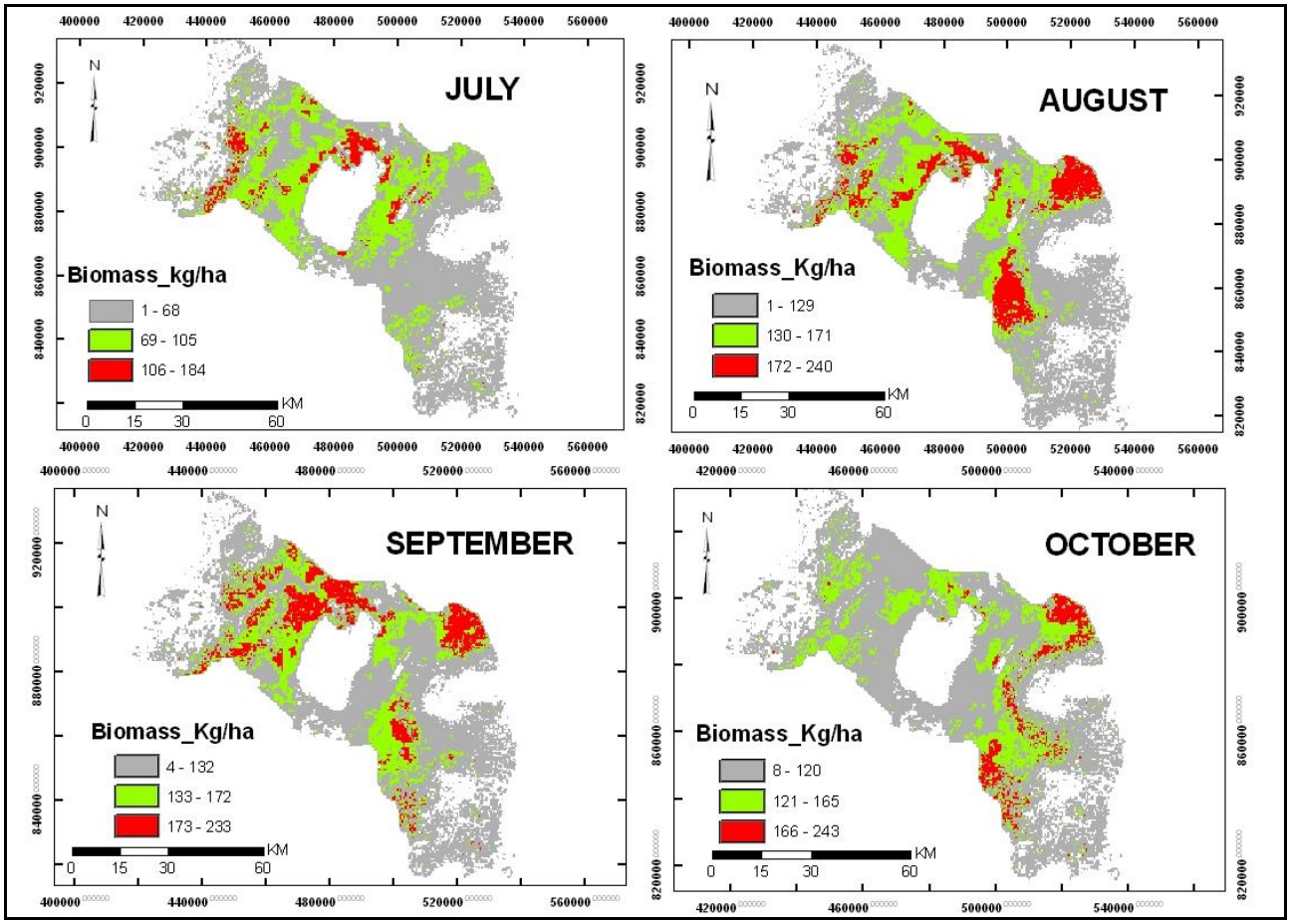

Figure 16 Profile of biomass production on summer season period of 2005

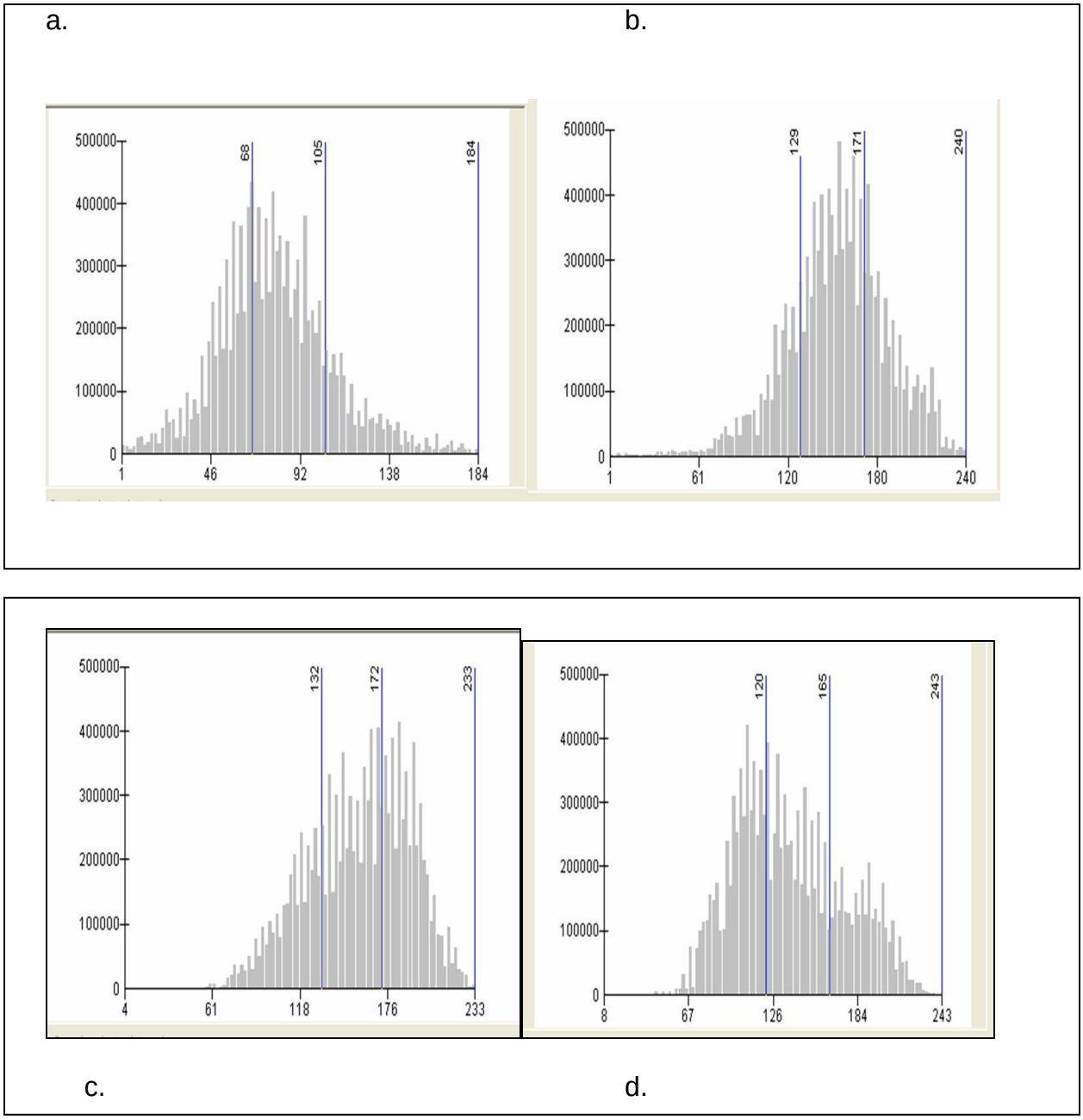

X-axis represent Biomass production in Kg/ha and **Y**-axis is number of pixels (frequency)

Figure 17 Histogram distribution map of biomass in 2005 year of months in a) July b) August c) September d) October Months.

8. Conclusion and Recommendations

8.1. Conclusion

In pervious studies, researchers used to estimate actual ET parameters from ground stationed meteorological data in the study area. Ideally, actual ET information (1) has sufficient spatial detail to enable analysis at the field level (2) covers large areas, such as entire river basins and (3) considers nonpristine growing conditions. Crop parameters including biomass growth have limitations to use their data for real time evaluation and analysis in the catchment scale. However, remotely sensing energy balance model, such as SEBAL can produce actual ET and biomass production that meet these requirements.

In the study area, daily and monthly actual evaporation in conjunction with biomass production have been computed for an area of 7380 km^2 employing SEBAL model.
The results of this study show that average evapotranspiration rates over the surface features in the area estimated on average that 1.7 mm/day and 40 mm/month (rift floor), 2.6 – 4.7 mm/day and 120 mm/month (in the escarpment and highlands) and 6 mm/day and 160 mm/month (Lake Ziway). Finally, actual ET determined from satellites yielding a spatio-temporal variation over the seasons. Moreover, biomass production over the cultivated land has been estimated using the model and the result on average showed that 150 Kg/ha. Biomass productions were increased when the actual ET inclined to higher value during September and October at the outlet of summer season and early stage of dry season when crops are at the end of maturity stage. Thus, frequent biomass determination from spectral data can be used for quick understanding of the crops situations for early warring and planning purpose on the agricultural sector.

SEBAL can be applied and implemented for solving water resource and crop related parameters. It is anticipated that SEBAL can help in establishing the

1) Relation ships between lands uses and water use for the catchement:
2) Monitoring biomass growth of vegetation systems in the catchement.

8.2. Recommendation

- Analyze more hydrological years, with cloud free satellite images and better ground data: aerial actual evapotranspiration can be estimated using SEBAL model. This model application can be extended to evaluate hydrologic water balance at basin level.

- To Study the actual ET for an appropriate water management at the farm and the irrigated project level it is good to use high resolution imageries like ASTER (15m in 3 visible near infrared bands and 90m in 5 TIR band from 8.1 to 11.6micro meter) allow to combine with high temporal resolution (like MODIS).

- Calibrate ET and biomass production for each land cover unit and comprehensively verify and validate SEBAL outputs helps to improve its accuracy under several climatic conditions at field scales.

- Estimation of biomass production assessment is possible using remote sensing for a given climate condition. Therefore potential yield estimation can be further estimated for a standard crop using harvest index developed by Zwart and Bastiaanssen (2000).

References

Allen, R.G., Bastiaanssen, W.G.M., Tasumi, M., Morse, A., (2001). Evapotranspiration on the watershed scale using the SEBAL model and Landsat images, ASAE Meeting Presentation, Paper Number 01-2224, Sacramento, California, USA, July 30– August 1, 2001.

Bastiaanssen , W.G.M (1995), Regionalization of surface water flux densities and moisture indicators in composite terrain ,a remote sensing approach under clear skies condition in Mediterranean climate, Ph.D.thesis,271 pp, Wagenigen Agri. Univ.,Dep.of Water resource .,Netherland.

Bastiaanssen W.G.M, Menenti M, Feddes RA,Holtslag AA,(1998a). A remote sensing surface energy balance algorithm for lands(SEBAL) . int Journal of hydrology, 212-213

Bastiaanssen, W.G.M., and Ali, S., (2003). A new crop yield forecasting model based on satellite measurements applied across the Indus Basin, Pakistan. Agriculture, Ecosystems and Environment, 94:321-340

Bastiaanssen, W.G.M., E.J.M. Noordman, H. Pelgrum, G. Davids and R.G. Allen, 2005. SEBAL for spatially distributed ET under actual management and growing conditions, ASCE J. of Irrigation and Drainage Engineering 131(1): 85-93

Boccalletti M., Bonini M., Mazzuoli R., Bekele Abebe, Piccardi L., and Tortoric L. (1998) Quaternary oblique extensional tectonic in the Ethiopia rift (Horn of Africa). Tectonophysics 287:97-116.

Brutsaert W. and Sugita M., Application of selfpreservation in the diurnal surface energy budget to determine daily evaporation, Journal of Geophysical Research 97, No. D17, 1992, p. 18337-18382

Casanova, D., Epema, G.F., and Goudriaan, J., (1998). Monitoring rice reflectance at field level For estimating biomass and LAI. Field Crops Res., 55:83-92.

Dagnachew Legesse, C. Vallet-Coulomb,F.Gasse(2003). Hydrological response of a catchement to climate and land use changes in tropical Africa ; case study south central Ethiopia ,J.hydrol,275;67-85.

De Bruin H.A.R. and Holtslag A.A.M., A simple parameterization of the surface fluxes of sensible andlatent heat during daytime compared with the Penman-Monteith concept, Journal of Applied Meteorology, 21, 1982, p. 1610-1621.

De Wit, C.T.(1965) photosynthesis of Leaf Canopies, Verslag Landbouwkunding Onderzoek (Ag.Research Rep.)nr.663.Wageningen.pudoc.

Ethiopia Mapping Authority, 1982.

Ethiopia Meteorological Service, 2004/2005.

Gasparon M., Innocenti F., Manetti P., Peccerillo A., Tsegaye A (1993). Genesis of the Pliocene to recent bimodal Mafic-felsic volcanism in the Debre Zeit area; central Ethiopia. Volcanological and geochemical constraint. Jour.Afri.Eart.Scie. 17(2); 145-165.

Gilabert, M.A., and Melia, J., (1990). Usefulness of the temporal analysis and normalized difference vegetation in the study of rice by means of Landsat-5 TM images: Establishment of relationship for yield prediction purpose. Geocarto Int., 5(4):27-32.

Jackson R.D., Moran M.S., Gay L.W. and Raymond L.H., Evaluating evaporation from field crops using airborne radiometry and ground-based meteorological data, Irrigation Science 8, 1987, p 81- 90.

Kumar, M., and Monteith, J.L. (1981). Remote sensing of plant growth. In plant and daylight spectrum (P.A. Huxley, Ed), International Council for Research in Agro-foestry, Nairobi, pp 347-364.

Kustas W.P. and Daughtry, Estimation of the soil heat flux/net radiation ratio from spectral data, Agricultural and Forest Meteorology 49, 1990, p. 205- 223

Mengesha Teferra, Tadiwos Chernet and Werkineh Haro (compiler), (1996): Geological Map of Ethiopia, scale 1:2,000,000, 2nd edition and explanatory note, Bulletin No. 3, GSE.

Mohr P (1962) Surface cauldron subsidence and associate Faulting and fissure basalt at Gariboldi pass; shoa. Bull. Volc.24

Mohr P (1971) The Geology of Ethiopia , Addis Ababa University Press.

Monteith, J.L., (1972). Solar radiation and productivity in tropical ecosystems, J. Applied Ecology, 9:747-766.

Moran, S.M., Jackson, R.D., (1991). Assessing the spatial distribution of evaporation using remotely sensed inputs. J. Environ. Qual. 20, 725–737.

Prince, S.D. (1990) High temporal frequency remote sensing of primary production using NOAA-AVHRR data .pp 169- 184. In book Application of Remote sensing in Agriculture (Eds. M.D.Stevene and J.A.Clark). Butterworth.

Robert L.Laury and C.C Albritton (1975). Geology of middle stone age Archaeological sites in the main Ethiopia rift valley south Methodist Univ, Dep. Geol.SCi V.86, No.7, pp 999-1011.

Street F.A., (1979). Late Quaternary Lakes in the Ziway-Shala Basin, southern Ethiopa. (UK).PhD Thesis Quaternaire;STR-80.094

Tenalem Ayenew, (1998) The hydrogeological system of the lake district basin central main Ethiopia Rift. PhD thesis ITC publication no.46 The Netherlands.

Tenalem Ayenew, (2003). Evapotranspiration estimation using thematic mapper spectral satellite data in the Ethiopia rift and adjacent highlands. Journal of hydrology, 279(1-4); 83-93.

Tesfaye Korme, Chorowicz J., Collet B and Bonavia F (1997). Volcanic vents rooted on extension fracture and their geodynamic implication in the Ethiopia Rift. Journal of volcanology and geothermal research 79; 205-222.

Tesfaye Cherent, (1982). Hydrogeological map of the Lakes regions(with memo). Ethiopia institute of Geological Surveys, Addis Ababa, Ethiopia.

Wiegand, C., Shibayama, M., Yamagata, Y., and Akiyama, T. (1989). Spectral observations for Estimating the growth and yield of rice. Jpn. J. Crop Sci., 58(4):673-683.

Woldegebriel, G., Aronson, J.L., Walter, R.C., (1990). Geology, Geochronology, and rift basin development in central sector of the Main Ethiopia Rift. Geol.Soc.Am. Bull.102,439-458.[B34.022]

Zhong, Q., Li, Y.H., (1988). Satellite observation of surface albedo over the Qinghai-Xizang plateau region. Adv. Atmos. Sci. 5, 57–65.

Zwart, S & Bastiaanssen W.B.M, (2004). Review of measured crop water productivity values for irrigated wheat, rice, cotton, and maize. Agricultural Water Management 69: 115-33.

Annex 1 Daily Evapotranspiration at Ziway station (Penman Monteith)

Year	Jan1st	Feb9th	Mar22th	May20th	Jan8th	Jul1th	Oct19th	Nov25th	Dec4th
2004	4.9	4.3	5.9	4.9	6.0	5.1	5	4.7	4.2

Annex 2 Monthly Evapotranspiration at Ziway station (Penman Monteith)

Year	Jan	Feb	Mar	Apr	May	Jun	Jul	Aug	Sep	Oct	Nov	Dec
2004	132	132	148	144	154	150	122	123	122	140	134	132

Annex 3 Monthly Evapotranspiration at Meraro station (Penman Monteith)

Year	Jan	Feb	Mar	Apr	May	Jun	Jul	Aug	Sep	Oct	Nov	Dec
2001			99.33	120.73	118	67.624	63.031	54	97	118	151.9	178.6
2002	182.2	250	130.5	120.4	158	91.924	80.9	63	103	137	189.6	109.4
2003	160.4	208	232.0	144.8	183	102.2	43.6	53	75	126	166.1	162.6
2004	161.5	212	171.9	73.6	181	88.7	44.4			96.8	112.0	131.0

Annex 4 Monthly Evapotranspiration at Bui station (Penman Monteith)

Year	Jan	Feb	Mar	Apr	May	Jun	Jul	Aug	Sep	Oct	Nov	Dec
1990	167.1	73.5	108.7	97.1	146.5	110.1	68.8	65.1	81.1	169.4	144.3	165.7
1991	157.0	124.2	102.8	198.6	154.4	12.2	57.0	57.2	95.4	189.9	188.0	174.6
1992	129.3	109.4	207.0	174.6	142.5	124.1	66.9	58.5	90.2	29.6		
1993						90.4	51.0	56.0	62.6	100.0	134.8	175.0
1994	189.8	180.5	176.6	199.4	201.7	72.3						
1995												
1996	127.0	191.6	129.8	163.3	85.5	70.5	63.8	68.6	87.3	194.6	194.0	195.3
1997	156.9		222.1	142.3	222.8	143.9	86.1	92.4	136.5	160.9	132.0	190.3
1998	141.3	126.9	177.0	219.9	171.6	145.3	75.9	67.3	89.0	117.7	175.2	227.7
1999	206.7	163.6	183.4	247.8	221.2	29.0	91.8					
2000	273.0	280.4	291.3	227.1	201.6	150.8	87.2	73.7	87.0	131.2	153.6	151.7
2001	169.5	212.7	133.1	201.8	131.9	98.7	69.3	90.6	138.9	199.4	198.7	196.8
2002	161.9	309.9	192.4	225.6	186.2	125.4	128.4	97.7	127.6	225.6	246.5	143.5
2003	177.9	103.0	234.6	169.1	209.3	132.9	96.3	80.7	109.4	201.9	201.1	168.0
2004	169.6	229.5	250.1	153.4	255.1	147.1	104.8	84.8	109.3	186.0	231.8	193.1
2005	180.6	258.5	195.4	195.4	130.2	113.9	945.5	86.6	105.9	185.3	231.4	253.4

Annex 5 Actual Evaporation on the basis of catchement physiography

Methods	Phys.area	Jan	Feb	Mar	Apr	May	Jun	Jul	Aug	Sep	Oct	Nov	Dec
Thornwaite	High land	41	57	83	95	94	91	84	78	83	74	52	35
	Escarpment	38	53	81	94	91	97	90	86	91	63	54	34
	Rift floor	20	36	56	70	66	78	109	101	95	63	22	14
	Weigh	37	53	78	91	89	91	90	84	87	70	48	32
Penman	High land	40	54	87	97	95	87	67	77	87	88	65	38
	Escarpment	33	49	80	92	90	97	79	81	90	86	60	34
	Rift floor	19	35	55	69	66	78	101	104	95	63	25	14
	Weigh	35	50	80	92	89	88	75	82	89	84	58	33

Source: Tenalem Ayenew (2003)

Annex 6 Estimation of open water evaporation with different methods in (mm)

Lake	Method	Jan	Feb	Mar	Apr	May	Jun	Jul	Aug	Sep	Oct	Nov	Dec	SEBAL
Ziway	Penman	150	128	148	188	188	135	139	135	164	200	223	225	150 (Jan)
	Radiation	135	120	142	138	138	107	115	115	124	151	157	157	
	Pan	159	144	192	142	156	137	126	123	112	170	178	130	

Source: Tenalem Ayenew (2003)

Annex 7 Maximum Active incoming short wave radiation (Rsn in Cal/cm^2 /day) and Gross dry mass matter Production on Overcast ($Y_{o)}$ and clear days (Yc) in Kg/ha/day for standard crop.

North South	Jan July	Feb Aug	Mar Sep	Apr Oct	May Nov	Jun Dec	Jul Jan	Aug Feb	Sep Mar	Oct Apr	Nov May	Dec Jun
O^0 Rsn	343	360	369	364	349	337	343	357	368	365	349	337
Yc	413	424	429	426	417	410	413	422	429	427	418	410
Yo	219	226	230	228	221	216	218	225	230	228	222	216
10^0 Rsn	299	332	359	375	377	374	375	377	369	345	311	291
Yc	376	401	422	437	440	440	440	439	431	411	385	370
Yo	197	212	225	234	236	235	236	235	230	218	203	193
20^0 Rsn	249	293	337	375	394	400	399	386	357	313	264	238
Yc	334	371	407	439	460	468	465	451	425	387	348	325
Yo	170	193	215	235	246	250	249	242	226	203	178	164
30^0 Rsn	191	245	303	363	400	417	411	384	333	270	210	179
Yc	281	333	385	437	471	489	483	456	412	356	299	269
Yo	137	168	200	232	251	261	258	243	216	182	148	130

Annex 8 crop development stages of major crops

Type of crop	Crop development stages				
	Initial	Development	Mid season	Late season	Total growing days
Maize	25	40	45	30	140
Onion	15	25	70	40	150
Pepper	25	35	40	20	125
Potato	25	30	45	30	130
Tomato	30	40	40	25	135
Millet	20	30	55	35	140
Carrot	20	30	30	20	100
Wheat	15	30	65	40	150